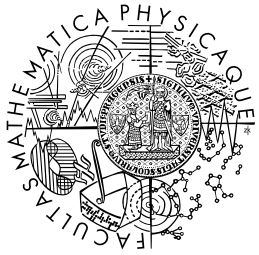

FACULTY
OF MATHEMATICS
AND PHYSICS
Charles University

DOCTORAL THESIS

Tomáš Pazderka

Study of protein structure and dynamics by means of optical spectroscopy

Institute of Physics of Charles University

Supervisor of the doctoral thesis:	RNDr. Vladimír Kopecký, Ph.D.
Consultants:	RNDr. Kateřina Hofbauerová, Ph.D., Prof. RNDr. Vladimír Baumruk, DrSc.
Study programme:	Physics
Study branch:	Biophysics, Chemical and Macromolecular Physics

Prague 2018

I declare that I carried out this doctoral thesis independently, and only with the cited sources, literature and other professional sources.

I understand that my work relates to the rights and obligations under the Act No. 121/2000 Sb., the Copyright Act, as amended, in particular the fact that the Charles University has the right to conclude a license agreement on the use of this work as a school work pursuant to Section 60 subsection 1 of the Copyright Act.

In Prague, July 3, 2018 Tomáš Pazderka

Title: Study of protein structure and dynamics by means of optical spectroscopy

Author: Tomáš Pazderka

Institute: Institute of Physics of Charles University

Supervisor: RNDr. Vladimír Kopecký, Ph.D., Institute of Physics of Charles University

Abstract: The aim of this thesis is to improve understanding of protein structure and dynamics and extend experimental setup and data processing for such studies. We focus on the extension of experimental feasability of vibrational optical activity (VOA). We have demonstrated a usability of intensity calibration in the field of Raman optical activity. Advantages for measurements on multiple instruments and/or using different configurations have been shown. A new instrumental setup has been developed for microsampling measurements of vibrational circular dichroism spectra with a spatial resolution of 1 mm. Using this technique, spatial inhomogeneities in a sample of protein fibrils have been observed. Model compounds for amide nonplanarity have been investigated utilizing several methods of optical spectroscopy and key spectral features for determination of amide nonplanarity and the absolute configuration have been identified. A comprehensive set of Raman spectra of proteinogenic amino acids has been measured. Sample concentration dependencies and consequent phase transitions have been identified and discussed. Decision rules for two-dimensional correlation analysis (2DCoS) have been extended to bisignate spectra. 2DCoS for model VOA (bisignate) spectra have been computed and analysed. A process of protein oligomerization has been studied utilizing vibrational spectroscopy and 2DCoS. Differences in behaviour of two phenotypes of human haptoglobin have been studied using hetero-sample 2DCoS. Dynamics of α_1-acid glycoprotein and its complex with a ligand has been investigated using Raman spectroscopy and principal component analysis. Differences in behaviour of both systems have been identified and discussed. Process of protein fibrillation in H_2O/D_2O has been investigated using vibrational circular dichroism and bands arising from amide I vibrations have been identified.

Keywords: two-dimensional correlation analysis, peptides and proteins, vibrational optical activity, structure and dynamics

I would like to thank my supervisor Dr. Vladimír Kopecký. I am very grateful for his guidance, interest and encouragement. Great thanks go to my consultant Dr. Kateřina Hofbauerová. Her advice and help with sample preparations were very valuable. My thanks go to Prof. Vladimír Baumruk for sharing his expertise in the field of ROA spectroscopy, for his encouragment and support.

I would also like to thank Prof. L. A. Nafie and Dr. Rina K. Dukor for guiding me during my internship at BioTools, Inc., FL, U.S.A. I am very grateful that they shared their great expertise in the field of VOA spectroscopy with me and allowed me to participate on a development of VCD microscopy. I would like to thank Prof. I. K. Lednev for guiding me during my internship at the University at Albany, State University of New York, NY, U.S.A and Dr. M. Shanmugasundaram for sharing his knowledge of AFM and deep-UV resonance Raman spectroscopy measurements.

I would like to thank Dr. Lucie Bednárová for her valuable advice in the field of vibrational spectroscopy and for her immense patience.

I would also like to thank all of my colleagues in the laboratory, mainly to the head of the department, Prof. Josef Štěpánek, for his help, encouragment and support.

The Charles University Grant Agency (project no. 560612) is acknowledged for providing me with financial support.

Finally, I would like to thank my family, especially my parents and my wife Markéta for their support and encouragement.

Contents

Preface

Proteins perform a large number of functions in living organisms, including molecular transport, regulation of cellular processes, cellular movement and many others. They also serve as basic building blocks of cells. Structure of proteins and their dynamical behaviour is directly connected to their function. If we want get better understanding of protein function, we have to investigate their structural and dynamical properties. This is one of the key tasks of molecular biology and various techniques can be used for this purpose.

Vibrational spectroscopy has been already proved to be a valuable tool for studying protein structure. Although the resolution of vibrational spectroscopy is lower than for the alternative methods, such as nuclear magnetic resonance (NMR), X-ray diffraction or electron microscopy, it is less demanding and its measurements are relatively easy to set up. Its advantage include a possibility of measurements in aqueous solutions, sensitivity to structural details, non-destructivity and no upper limit for the size of studied molecules. When an external perturbation is applied to the studied systems, vibrational spectroscopy methods even enable investigation of the dynamic behaviour and response of the systems to the external perturbation. When combined with chiroptical spectroscopies (vibrational circular dichroism (VCD) or Raman optical activity (ROA)), vibrational spectroscopy can provide us with even more detailed information about the underlying protein structure and dynamics.

The goal of this dissertation thesis is to get better understanding of protein structure and dynamics and extend the methodology for such studies. We have focused on a development and extension of the experimental feasibility of vibrational optical activity (VOA). As a part of this work, intensity correction protocol for ROA experiment has been established, VCD instrumentation has been modified to allow microscopic measurements and application of two-dimensional correlation spectroscopy (2DCoS) on VOA spectra has been improved. All these improvements have been tested on protein samples.

The thesis is organized as a collection of papers with a short introductory commentary divided into two chapters. The first chapter contains a brief introduction to the methods and studied systems and is divided into four parts. The first part concentrates on proteins, their structure, and dynamics. The second part describes the methods of vibrational spectroscopy and their applications to protein studies. The third part contains basics of 2DCoS and the last part describes the use of principal component analysis (PCA) in molecular spectroscopy. The second chapter contains a summary of the achieved results and is divided into two parts. The first part summarizes the results on methodology improvements and studies of model systems. It involves (i) utilization of spectral intensity corrections for VOA studies; (ii) a development of instrumentation for VCD microsampling; (iii) studies of amide nonplanarity on model compounds; (iv) analysing a comprehensive spectral set of amino acids measured by Raman spectroscopy. The second part presents studies of dynamical behaviour of proteins using the described techniques and involves (i) an extension of 2DCoS to VOA

spectra and proper treatment protocols; (ii) studies of protein oligomerization using vibrational spectroscopy and 2DCoS; (iii) a study of ligand binding influence on protein stability; (iv) a study of process of protein fibrillation observed by VCD.

1. Introduction

1.1 Proteins, their structure and dynamics

Proteins are large, complex biological molecules which can be found in all living organisms [1]. They are composed of amino acids linked by peptide bonds. There are 20 proteinogenic amino acids which are directly encoded in the genetic code and additional 2 amino acids that can be incorporated via special translational mechanism [2].

The amino acids have different functions in proteins and can be found in various locations. For example, cysteine can form a disulphide bond with another cysteine and covalently connect two parts of the protein. They can even link two different chains to stabilise a protein dimer. Glycine, having no side chain, can add flexibility to the protein chain. Proline is a tertiary amide and thus forces a bend in the polypeptide chain. Serine and threonine usually serve as hydrogen donors in enzymes. Hydrophobic amino acids (phenylalanine, leucine, isoleucine, and valine) usually form a hydrophobic cavity inside the protein which can serve as an active site. Methionine contains methyl group attached to a sulphur atom, which can be activated and is involved in reactions adding a carbon atom to another molecule [3].

1.1.1 Structure

We recognize four levels of protein structure. The primary structure is given by an amino acid sequence, secondary structure is determined by local structural conformations which are held together by hydrogen bonds between C=O and N–H. Tertiary structure is the overall three-dimensional arrangement of the secondary structure features and the quaternary structure is given by an interaction of individual protein chains (subunits).

There are four main types of secondary structures – β-sheets, helices, turns and coils [1]. Available secondary structures are constricted by the accessible angles of the peptide bond [4]. Amino acids in helices are arranged in a helical structure where the number of residues per turn and the number of atoms involved in a ring formed by a hydrogen bond varies. The most common type of helical structure is a right-handed 3.6_{13}-helix, also known as α-helix. Other types include a right-handed 3_{10}-helix and 4.4_{16}-helix (also known as π-helix). A twist of the helical structure can be either right- or left- handed, although the former is more prevalent in proteins. A representative of the latter is a poly-proline II helix (PPII) occurring in proteins comprising of repeating proline residues. PPII is typically present in intrinsically disordered proteins and unordered proteins [5].

β-sheets are composed of β-strands which are connected by backbone hydrogen bonds. They are usually twisted and can be either parallel, where the strands are all oriented in the same way, or antiparallel with alternate orientation of each strand.

Turns are secondary structure elements which serve to reverse polypeptide chain direction. Based on a distance between two end residues, several types

of turns are recognized. The most common types include β-turns, loops, and hairpins.

Coils are a class of conformations with the polypeptide chains oriented randomly while still retaining hydrogen bonds to adjacent residues.

A relative arrangement of individual secondary structure elements is called tertiary structure. Individual parts of the protein can be held together by disulphide bonds, hydrogen bonds, salt bridges or non-polar hydrophobic interactions.

Quaternary structure is important for large protein assemblies. The most common assemblies are protein dimers but larger structures such as tetra- or hexamers can occur as well. The most notable exceptions are large molecular machines – proteasome, spliceosome, ribosome or transcription complex.

1.1.2 Dynamics

Protein structure is not a static arrangement but it can change in response to a change of external conditions or due to interactions with other molecules. This dynamical behaviour is crucial for some of the protein functions. The changes in protein structure can enable ligand binding, transfer of molecules, trigger signalling pathways or catalysis [6, 7]. Investigation of protein structure and dynamics is important for better understanding of protein function or the eventual malfunction. Studies of diseases related to protein misfolding might enable development of drugs targeting specific protein-related diseases.

Protein dynamics can involve several residues or whole protein subunits. In some cases, even a small change of amino acid side chain conformation could alter a hydrophobic cavity inside a protein and thus allow or prevent ligand binding. In other cases, structural elements such as α-helices or β-sheets can relax, contract or bend and thus change the overall shape of the protein. It is also possible to observe hinges in proteins [8], enabling whole domains to move and open/close cavities [9]. In large molecular machines, it is rather common for whole subunits to change their position and/or shape [10].

Under some conditions, proteins can denature and, as a consequence, can no longer perform their function. Denatured proteins are then disassembled by cellular pathways and the individual amino acids are recycled. Under certain conditions, proteins can attain a fold in which they cannot be broken down by these mechanisms and they can also induce the same fold for other proteins [11], see fig. 1.1. They then form aggregates or, eventually, plaques around cells and can prevent their normal function. These deposits are called amyloids and are usually comprised of β-sheet-rich proteins forming long fibrils [12]. Amyloid aggregates are often associated with neurodegenerative diseases such as Parkinson's disease, Huntington's disease and prion diseases [11].

Protein dynamics cannot be easily studied by X-ray and, for large systems such as fibrils, NMR studies are also difficult. On the other hand, detailed information about protein structural changes can be obtained by the methods of optical spectroscopy, which are not limited by the size of the studied systems. The richness of information provided by the methods of vibrational spectroscopy and their sensitivity to detail makes them especially suitable for protein dynamics studies.

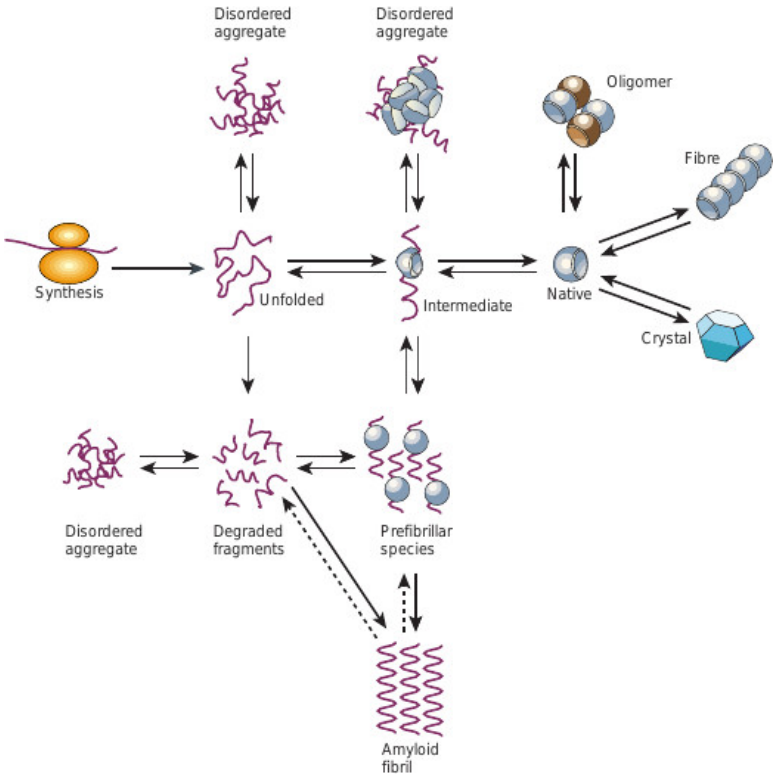

Figure 1.1: Possible pathways for protein in living cells. Taken from Dobson [11].

1.2 Vibrational spectroscopy of proteins

Vibrational spectroscopy is a branch of molecular spectroscopy that probes vibrational energy levels of molecules using absorption or scattering of incident light fig. 1.2. There are two basic vibrational spectroscopy methods: infrared (IR) spectroscopy and Raman spectroscopy. In IR spectroscopy, the sample is irradiated by a polychromatic light which is absorbed if the light energy matches the energy of vibrational transition. In Raman spectroscopy, a sample is irradiated by a monochromatic light and the photons are inelastically scattered. The gained/lost energy is then the energy of the vibrational transition.

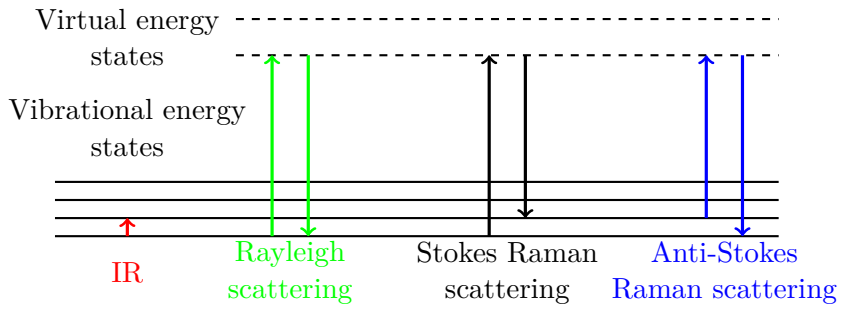

Figure 1.2: Energy level diagram for vibrational spectroscopies

Vibrational spectroscopy can provide us with a valuable insight into protein structure without the need of crystallization or isotopic labelling. It is also possible to measure proteins in water solution which is their natural environment

[13]. Vibrational spectroscopy can also be used for probing a state of the amino side chains [14]. Moreover, the short timescale of vibrational transitions allows us to sample individual conformers in the protein population. It is also possible to apply external perturbation and study protein response and dynamics.

Information obtained by the vibrational spectroscopy methods can be enhanced with spectroscopic techniques of VOA. VOA provides us with rich structural information by means of interactions of molecules with left circularly polarized (LCP) and right circularly polarized (RCP) light. The VOA counterpart of IR spectroscopy is VCD and for the Raman spectroscopy, the counterpart is ROA [15].

1.2.1 Infrared spectroscopy

Application of the IR spectroscopy in the field of aqueous solutions of biomolecules is, in general, complicated by the fact that H–O–H bending vibrations of H_2O absorb very strongly around 1640 cm^{-1} – as a consequence, cells with very short pathlengths of 6–10 μm are needed for the transmission measurements (fig. 1.3).

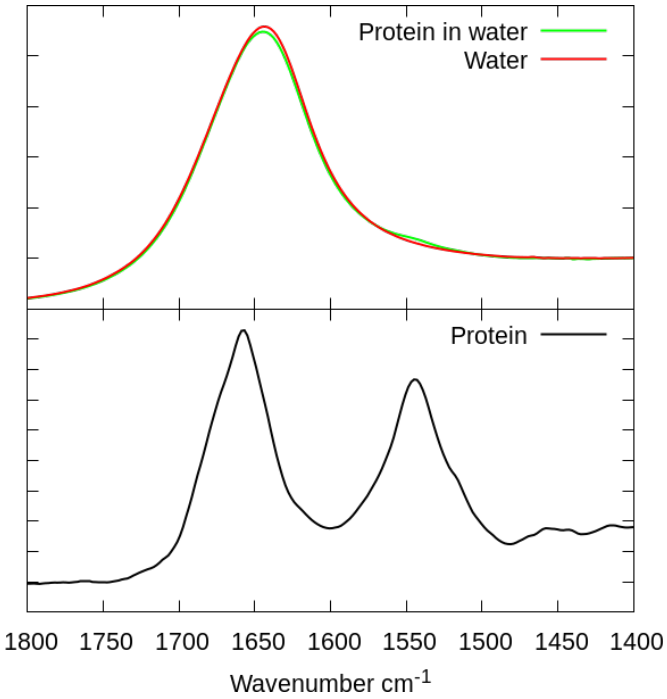

Figure 1.3: Top: typical IR spectra of protein in water solution (green) and water (red). Bottom: protein spectrum after water subtraction (black).

Consecutively, a relatively high protein sample concentration (∼10 mg/mL) is required for the measurements [16, 17]. Even though a strength of vibrating bonds and masses of vibrating atoms have a dominant effect on infrared spectra, the chemical structure of proteins cannot be deduced directly from the spectrum due to band overlaps. Nevertheless, some changes, e.g., of protonation stage of Asp, Glu, His or Tyr residues can be directly recognized in the infrared spectra of proteins [14]. In IR spectroscopy, analysis of the vibrations of the amino acid side chains is complicated by an intense vibration of the peptide backbone.

Efforts to understand the vibrations of the protein backbone date back to 1980s, when a simple model of the peptide linkage, N-methylacetamide, was first investigated in detail [18]. Vibrational analysis of this molecule revealed several characteristic group frequencies for the peptide linkage. These are now well understood and are referred to as the amide I–VII, and amide A and B vibrational bands [19, 20]. The most intense protein vibration band corresponds to the amide I band at $\sim$1650 cm^{-1}, arising mainly from the C=O stretching vibrations with a minor contribution from out-of-phase C–N stretching vibrations [19, 21]. The amide I vibrations are strongly affected by the secondary structure conformation, therefore, the amide I band is most commonly used for the secondary structure analysis [17, 22–25]. The second most intense infrared band in the spectra of proteins – amide II – arises mostly from N–H bending coupled with C–N stretching vibrations and it is observed at around 1550 cm^{-1} in H_2O and shifts to about 1450 cm^{-1} in D_2O. Its strong frequency shift upon deuteration is used to monitor H/D exchange during protein unfolding [19, 26]. Amide III band is also observable (with rather low intensity) in the range between 1220–1330 cm^{-1} and results from an in-phase combination of N–H bending and the C–N stretching with a small contribution of C=O in-plane bending and C–C stretching vibration [16, 19, 20, 26]. The band is very sensitive to the secondary structure [27] but its practical usage is complicated due to its low intensity and strong side chain contributions to the amide III region [14]. The rest of the amide bands is usually not accessible by IR spectroscopy in solution due to experimental limitations.

In summary, IR spectroscopy can provide low-resolution information about protein secondary structure changes (including protein fibrillation), protein dynamics (including ligand binding), and side chain conformational changes [14, 19, 26]. It is particularly suitable for an investigation of different forms of β-structures, protein aggregation, and fibrillation, because these formations show unique spectral patterns in the amide I spectral region [18, 28]. Its important advantage is that the spectra are not obscured by sample fluorescence (low excitation energy) which can enable such measurements even for fluorescent proteins.

1.2.2 Raman spectroscopy

Raman spectroscopy represents a counterpart of IR spectroscopy in the field of vibrational spectroscopy. It is a scattering phenomenon based on a two-photon process. An incident photon from a laser excites a molecule into a virtual state. At the same time, another photon is scattered from this virtual level. Thus, the frequency of Raman scattered photons is symmetrically displayed around the Rayleigh scattering line (and usually expressed as Raman shift in wavenumbers) as Stokes and anti-Stokes Raman scattering ([20], fig. 1.2). In contrast to IR spectroscopy, water represents a good solvent for Raman spectroscopy. Therefore samples can be measured in aqueous buffers and standard cells or even in capillaries suitable for low sample volume measurements. Nevertheless, fluorescence impurities, as well as fluorescence of the samples themselves (e.g., protein ligands or porphyrins), could hamper Raman spectroscopy measurements [29].

Similarly to IR spectra of proteins, vibrations of the peptide bond are also observable in Raman spectra. However, the spectra are dominated by vibrations of amide I and III. The amide II band is very weak and overlapped by

intense δCH_2 and δCH_3 vibrational bands [29, 30]. On the contrary, Raman amide III band is more intense than in IR spectra but is often confused with ring vibrations of aromatic side chains of amino acids. Compared to IR spectra, Raman spectra involve many intense bands arising from amino acid side chain vibrations [31]. Various Raman bands due to tyrosine [32], tryptophan [33, 34], histidine [35], phenylalanine and cysteine [36, 37] residues are readily visible and assignable and are commonly used to mark changes of protein tertiary structure as well as changes of environment of these amino acids [38]. Therefore, Raman spectroscopy possesses an informationally rich picture of protein structure and dynamics. However, relatively high protein sample concentrations are needed for the measurements ($\sim$10 mg/mL).

1.2.3 Drop coating deposition Raman spectroscopy

The above mentioned limitation of conventional Raman spectroscopy can be surpassed by an emerging technique of Raman spectroscopy – drop coating deposition Raman (DCDR) spectroscopy [39]. The method is based on the so-called "coffee ring effect" – the phenomenon recognized by theoretical physicists more than 20 years ago in suspensions like coffee, tea, wine, etc. [40]. The phenomenon arises from a capillary flow in water droplets at a hydrophobic surface, in which pinning of the contact line of the drying droplet ensures that the solvent that evaporates from the droplet edge is replenished by a liquid from the interior. The resulting flow carries all the dispersed material towards the edge of the droplet, where a ring of solute macromolecules is formed [41]. After the droplet evaporation, Raman scattering is collected from this ring containing an excess of deposited material [42]. Despite the fact that DCDR measurements may not be applicable to some of the protein samples as the formation of the ring can be prevented by a buffer or the sample itself, this method has been successfully implemented in the field of protein research, where the low sample volume (typically units of μL) and the possibility of protein analysis at low concentrations (down to μM) provide a substantial advantage [43, 44].

1.2.4 Vibrational circular dichroism

VCD is a chiroptical variant of IR spectroscopy measuring the difference in absorbance ($\Delta A = A_L - A_R$) of LCP and RCP infrared radiation, see fig. 1.4. This difference is non-zero only for chiral molecules. The first experimental observation was done by Holzwarth *et al.* [45] and the field has since expanded significantly. Nowadays, the main applications involve determination of absolute configuration of pharmaceutical molecules [46] and natural products [47] and conformational studies of important biological molecules, including proteins [48] and nucleic acids [49].

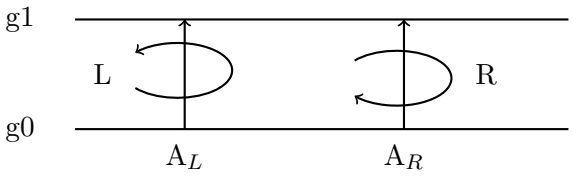

Figure 1.4: Schematic representation of VCD. g0 and g1 represent ground vibrational states.

For proteins, the main applications of VCD include conformational studies [50, 51], studies of binding with other biomolecules [52] and secondary structure estimation [50].

1.2.5 Raman optical activity

ROA is a chiroptical variant of Raman spectroscopy measuring the difference in scattering intensity ($\Delta I = I^R - I^L$) of RCP and LCP visible radiation (fig. 1.5). As for VCD, this difference is non-zero only for chiral molecular systems. The first experimental observation was done by Barron *et al.* [53] and since then the field has been growing [54–56]. Current applications are conformational studies of biological molecules, including proteins [57, 58] and nucleic acids [59] but ROA can be used even for large and complex structures, e.g., viruses [60].

Raman scattering is a two-photon process, and it is possible to detect/control the light chirality in both incident and scattered beams. This results in four different experimental schemes: incident circular polarization (ICP), where the incident beam is circularly polarized, scattered circular polarization, where the detection of circular polarization happens in the scattered beam and two variants of dual circular polarization where the chirality is present in both beams and is either the same, or opposite [61].

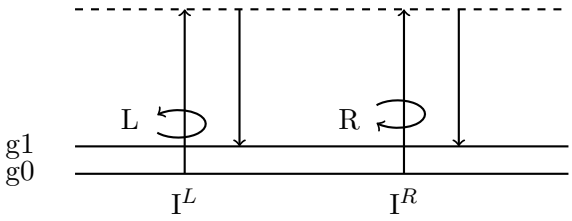

Figure 1.5: A schematic representation of ROA in the ICP scheme.

Chiral response of the studied systems brings an extra sensitivity, making the methods of VOA especially suitable for the studies of chiral biomolecules. Since VOA spectra are usually rather complicated and contain many complex features, it might be advantageous to utilize methods of multivariate statistics and/or 2DCoS for detailed data analysis.

1.3 Two-dimensional correlation analysis

2DCoS was invented by Prof. Isao Noda when studying dynamic infrared linear dichroism of polymer films [62]. Complicated interpretations of complex spectra

of the studied polymer systems – reflecting different spectral rates and overlapped spectral band responses – led to the idea of 2DCoS which was first presented in 1986 [63]. The path to acceptance of this method was rather long since the first article about 2DCoS was published in 1989 [64]. The first featured article followed in 1990 [65].

2DCoS is a method that allows determination of sequential order of spectral changes in dependence on external perturbation [66, 67]. In order to perform a 2DCoS spectroscopy, an external perturbation (i.e., pH, temperature, time, or concentration) has to be applied to the studied system. This disturbed system is then studied by a selected spectroscopic technique (called probe – i.e., IR spectroscopy, Raman spectroscopy) in order to obtain a set of spectra with perturbation-induced changes.

Given a discrete set of measured data $y(\nu, t_j)$, where ν is a spectral coordinate and t_j is the external perturbation, we can derive a set of dynamic spectra $\tilde{y}_j$ as follows

$$\bar{y}(\nu) = \sum_{j=1}^{m} \frac{y(\nu, t_j)}{m} \tag{1.1}$$

$$\tilde{y}(\nu, t_j) = y(\nu, y_j) - \bar{y}(\nu) \tag{1.2}$$

$$\tilde{y}_j(\nu) = \tilde{y}(\nu, t_j) \qquad j = 1, 2, \cdots, m \tag{1.3}$$

where m is the total number of spectra in the measured set. Discrete orthogonal spectra $\tilde{z}_j$ can be obtained from

$$\tilde{z}_j(\nu_2) = \sum_{k=1}^{m} N_{jk} \cdot \tilde{y}_k(\nu_2) \tag{1.4}$$

where N_{jk} is so called Hilbert-Noda transformation matrix defined as follows:

$$N_{jk} = \begin{cases} 0 & \text{if } j = k \\ \frac{1}{\pi}(k - j) & \text{otherwise} \end{cases} \tag{1.5}$$

Using these modified spectra, we can calculate two parts of 2D spectra from the following formulas

$$\Phi(\nu_1, \nu_2) = \frac{1}{m-1} \sum_{j=1}^{m} \tilde{y}_j(\nu_1) \cdot \tilde{y}_j(\nu_2) \tag{1.6}$$

$$\Psi(\nu_1, \nu_2) = \frac{1}{m-1} \sum_{j=1}^{m} \tilde{y}_j(\nu_1) \cdot \tilde{z}_j(\nu_2) \tag{1.7}$$

where Φ is a synchronous part which represents simultaneous or coincidental changes and Ψ is an asynchronous part which represents successive or sequential changes [66].

Synchronous spectrum is always symmetrical with respect to the diagonal line ($\nu_1 = \nu_2$). Correlation peaks occur both on diagonal and off-diagonal locations. Peaks located on the diagonal are called autopeaks and their intensity corresponds to the autocorrelation function of spectral intensity. Off-diagonal elements, called cross-peaks, represent simultaneous or coincidental changes of spectral features

located at the corresponding frequencies. This suggests a possible relation of these changes. The sign of autopeaks is always positive but the sign of the cross-peaks can be either positive or negative. The positive sign means that the changes are both occurring in the same direction (both intensities are either decreasing or increasing – peaks at frequencies B and D in fig. 1.6) while the negative sign means that the changes are occurring in a reversed direction (peaks at frequencies A and C in fig. 1.6).

Asynchronous spectrum is always anti-symmetric with respect to the diagonal line and has no autopeaks. Asynchronous cross-peaks develop only if the spectral changes are out of phase with each other (delayed or accelerated). A sign of the cross-peak indicates the order of changes and is positive if the change at ν_1 happens before the change at ν_2 and negative if the change at ν_1 happens after the change at ν_2 fig. 1.6. This rule is reversed if the intensity of the synchronous spectrum at ν_1, ν_2 coordinate is negative. The model synchronous and asynchronous spectra in fig. 1.6 thus indicate that the changes at B and D positions occur before changes at A and C.

2DCoS is generally applicable to a broad range of analytical techniques such as IR spectroscopy, Raman spectroscopy, fluorescence, ultraviolet-visible spectroscopy, electronic circular dichroism, NMR and many others [66–68]. Nevertheless, IR spectroscopy is currently the most commonly used analytical probe in 2DCoS (about 57 % of the studies involve IR technique) [69]. Popularity of 2DCoS in IR spectroscopy is caused by a relatively low background variation of the spectra, their precise calibrations and relatively simple spectra processing. In contrast, Raman spectroscopy is used only in ∼10 % of the 2DCoS studies [69]. It is probably because of a relatively low signal to noise ratio (SNR), background variations, calibration shifts, and problems with sample fluorescence. There is an effort to keep the systems/probes simple for general applications of 2DCoS. The studied systems are not too complex and involve mainly polymers (about one third of studies), liquids, pharmaceuticals and bio-related compounds (also about one third). Complex samples such as proteins comprise less than 15 %. The most common external perturbations used in 2DCoS include temperature (representing about 38 %), time and concentration/pH-effects (applied in about 24 and 23 %, respectively) [69].

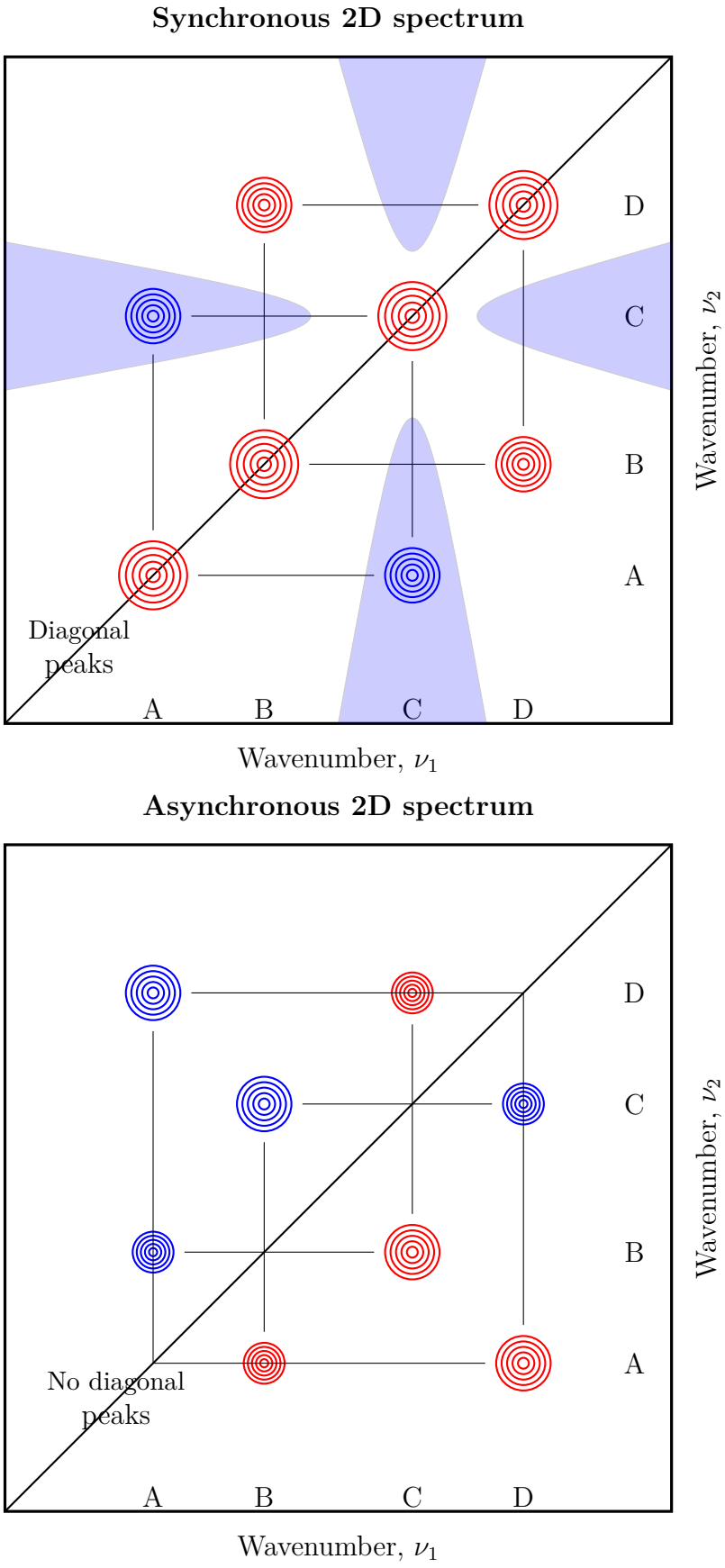

Figure 1.6: Schematic contour maps of synchronous (top) and asynchronous (bottom) 2D correlation spectra. Red contours represent a positive peak intensity and blue contours represents a negative peak intensity. Adapted from Noda and Ozaki [66]

1.4 Principal component analysis

PCA was invented in 1901 by Pearson [70] and later reinvented by Hotelling [71] in 1930s. It later gained a wide popularity and is now commonly used for data analysis in many fields of science, including astronomy [72, 73], food science [74, 75], medicine [76–78], and many more.

PCA is a method that allows reducing a set of multidimensional data by using an orthonormal transformation to convert observed data to a reduced set of unrelated components [79]. Each spectrum can be expressed as:

$$Y_i(\nu) = \sum_{j=1}^{M} V_{ij} W_j S_j(\nu), \tag{1.8}$$

where W_j is the diagonal matrix of singular values, V_{ij} is the unitary matrix of coefficients and $S_j(\nu)$ corresponds to the matrix of orthonormal subspectra. M represents the number of independent spectral series present in the analysed spectral set.

PCA can be used for a data set reduction [80]. A measured spectral series is deconstructed into individual components and only a few selected components are investigated. This can reduce the analysed spectral set size by several orders of magnitude. The number of considered spectra is selected in such a way that the reconstructed spectra explain the original dataset with a sufficient accuracy.

PCA can be also used to improve the SNR by applying a noise filter [76]. A higher SNR is achieved by applying a lossy compression on the data set. Data are deconstructed into subspectra. The subspectra which contain only random fluctuations and noise (with lowest singular values W_j) are discarded and the original spectral set is reconstructed again.

2. Results

2.1 Methodology

2.1.1 Relative intensity correction of ROA spectra

Performing ROA measurements on multiple instruments or utilizing different configurations of the same instrument may cause a problem with transferability of the collected data. Intensities of the measured spectra are influenced by optical parameters of the used components and by the experimental geometry and configuration. In order to qualitatively compare data measured on different ROA instruments or to compose a wide-range ROA spectrum from multiple snapshots taken on the same instrument, it is essential to perform an intensity calibration [81]. Several options are available for such calibrations. The most precise calibrations use a blackbody emitter [82] or a calibrated tungsten lamp [83].

We focused on a much cheaper and versatile alternative – a well characterized luminescent glass standard from the National Institute of Standard and Technology, U.S.A. (SRM 2242/2243 – NIST – see fig. 2.1).

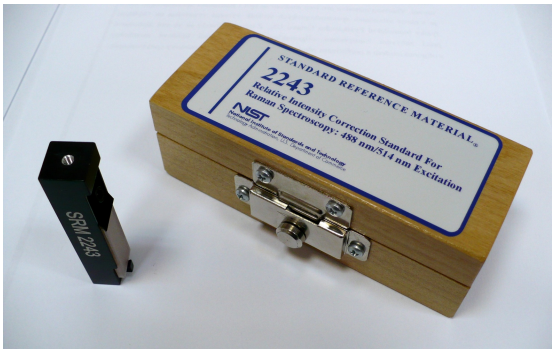

Figure 2.1: SRM 2242/2243 – NIST

Its usage is very simple and convenient [84]. The standards are available for a wide range of excitation wavelengths and they fit into standard cell holders so no modifications of experimental setup are necessary. First of all, a spectrum of the luminescent glass standard is measured for each instrument configuration. Theoretical spectrum is then constructed using polynomial expression supplied by a material manufacturer ([85], appendix 1). From these two spectra, a correction curve is created by dividing the theoretical spectrum by the measured luminescent spectrum (fig. 2.2). This correction factor is then applied alongside with a wavenumber calibration and assures correct relative peak intensities. We have demonstrated this approach on the samples of α-pinene and tricyclic spirodilactam measured using six different ROA instruments and their setups (varying gratings, scattering configurations – see fig. 2.3). As can be seen in fig. 2.4, the correction proves to be essential for comparing experimental data measured with different setups and also when comparing experimental and theoretical data. Thus, we practically demonstrated a simple applicability of the corrective procedure which significantly improves data quality, transferability, and reliability.

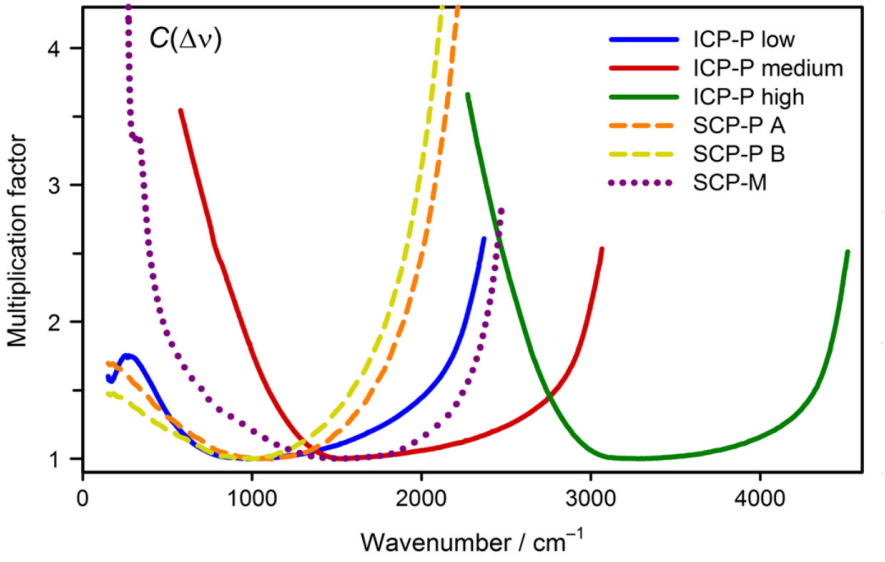

Figure 2.2: Calibration curves for three different ROA instruments (ICP-P, SCP-P, SCP-M) and their configurations.

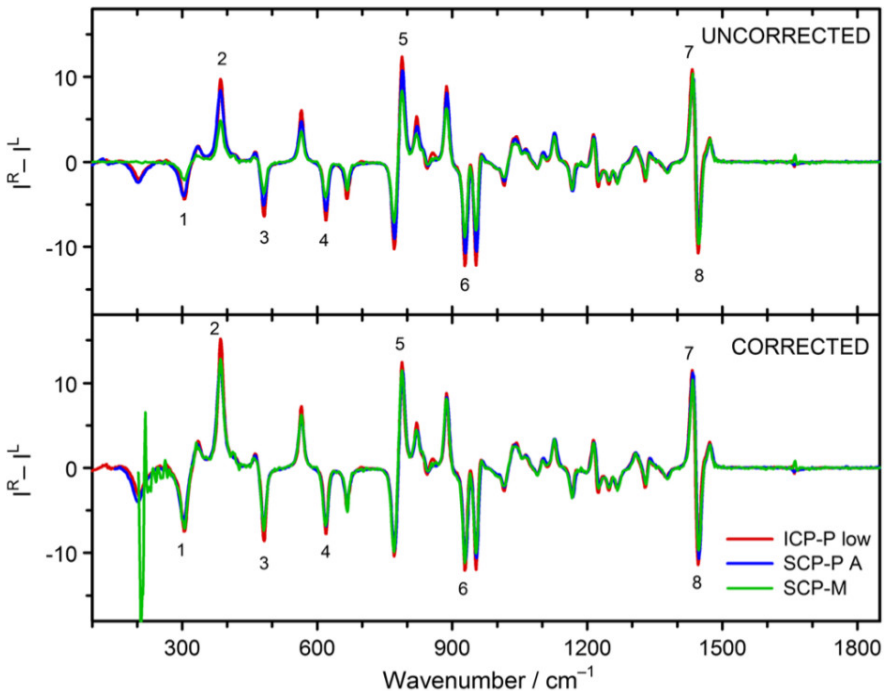

Figure 2.3: Uncorrected and corrected ROA spectra of (1R)-(+)-α-pinene measured on three different instruments and normalized to integral intensity within 1100–1400 cm^{-1}, where the effect of correction is minimal. The spectra are shown in the 100–1850 cm^{-1} interval where data from all three instruments were available.

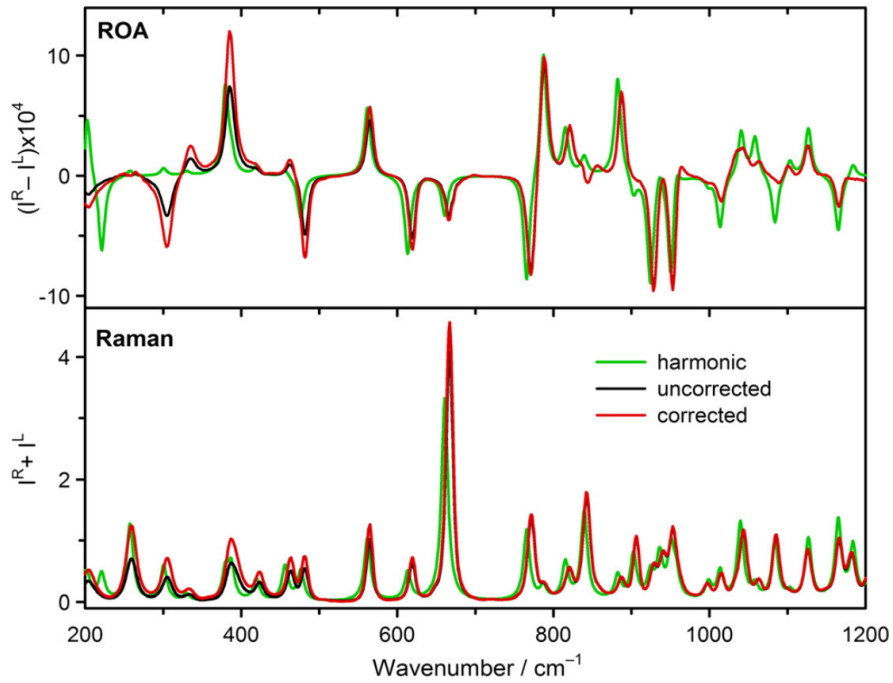

Figure 2.4: Experimental (corrected and uncorrected) and calculated (harmonic) Raman and ROA spectra of (1*R*)-(+)-α-pinene.

2.1.2 The development of VCD microscopy instrumentation

Within the last decade, VCD spectroscopy has proven to be a sensitive tool for detection of protein amyloid fibrils [86–89]. In VCD, protein fibrils are typically studied in solution. However, due to their very strong signal in VCD spectra, it could be even possible to detect amyloid fibrils in tissue samples and, consequently, study them *in vivo*. The biggest disadvantage for VCD studies of such biological samples is the fact that for commercial instruments a regular beam diameter is approximately 1 cm. VCD signal is then averaged over the whole area of the sample. Therefore, any spatial inhomogeneities of the sample are lost and only the most prevalent feature/structure is recognizable in the spectra. In order to gain more detailed information about the composition of the sample, we need to decrease the diameter of the probing beam.

For this purpose, we have modified a commercial VCD instrument (Chiral*IR*, BioTools, Inc.) for microscopic measurements. First, we placed a pair of $f/3$ lenses around the sample compartment in order to decrease the spot size down to ∼3 mm (fig. 2.5). To verify the SNR and estimate possible artefacts, a testing sample of α-pinene was measured. After verifying that the instrument was artefact-free and establishing the instrument throughput (88 % of the unmodified system), an amyloid fibril film was mapped using this resolution to scan for spatial inhomogeneities (fig. 2.6).

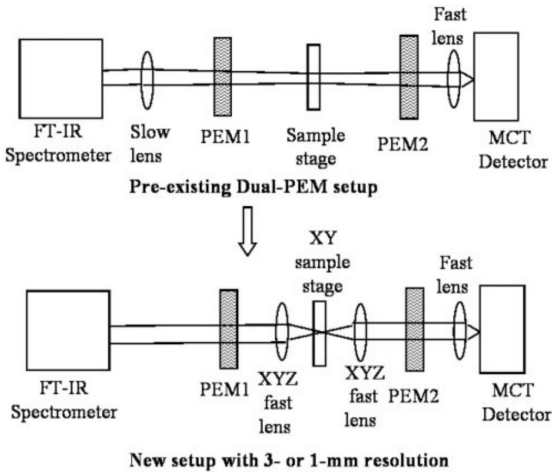

Figure 2.5: Diagram of the modified VCD setup for 3 or 1 mm resolution (below) adapted from the pre-existing VCD setup (above).

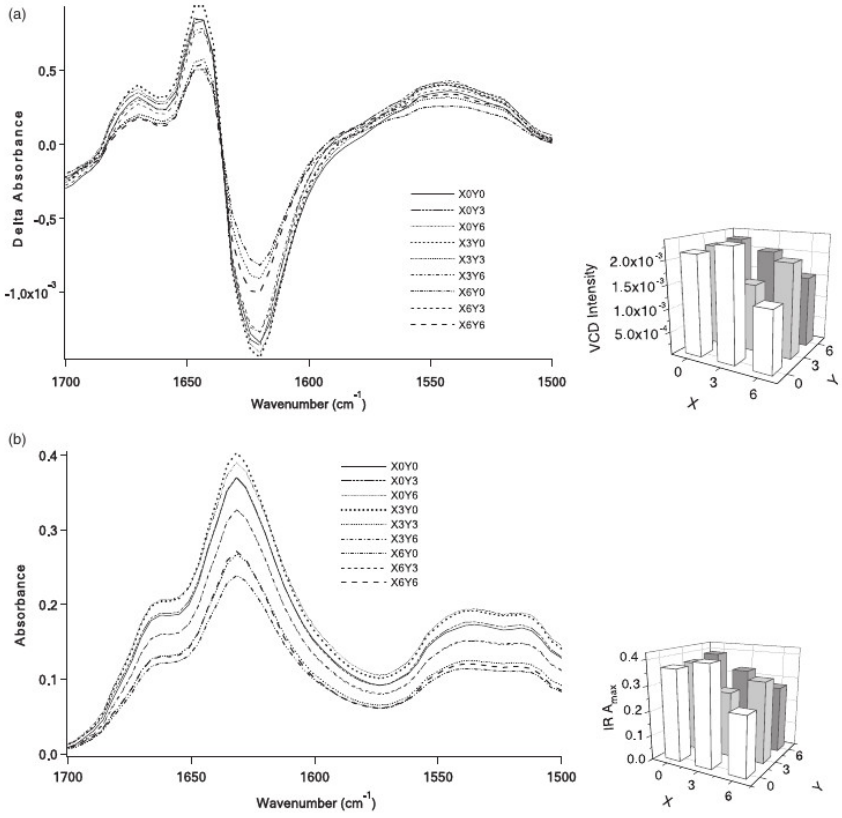

Figure 2.6: (a) VCD and (b) Fourier transformed infrared spectroscopy (FT-IR) spectra of an insulin fibril film at nine non-overlapping 3 mm spots across the film. The intensity of FT-IR absorbance maximum (A_{max}) and VCD intensity difference maximum ($\Delta A_{max} - \Delta A_{min}$) across the amide I and II regions are plotted for each of the nine different spots and shown to the right of the spectra. The FT-IR intensity map reveals different thicknesses of film deposit at different locations of the film. The similarity of the intensity change of VCD and FT-IR indicates that variation of film thickness is the primary reason for the change in intensity over the VCD map. The acquisition time is 5 min for each location.

In a next step, $f/3$ lenses have been replaced by $f/1$ lenses which further decreased the spot size down to $\sim$1 mm. The same testing sample was used for artefact and SNR evaluation. Again the setup was artefact-free and the throughput was established (50 % of the unmodified system). The same amyloid fibril film was mapped once again ([90], appendix 2, fig. 2.7). Despite the instrument throughput decrease, we have managed to perform a first VCD mapping of a biological sample. Further feasibility tests were performed on samples of human and animal tissues and cells (fig. 2.8 – unpublished results).

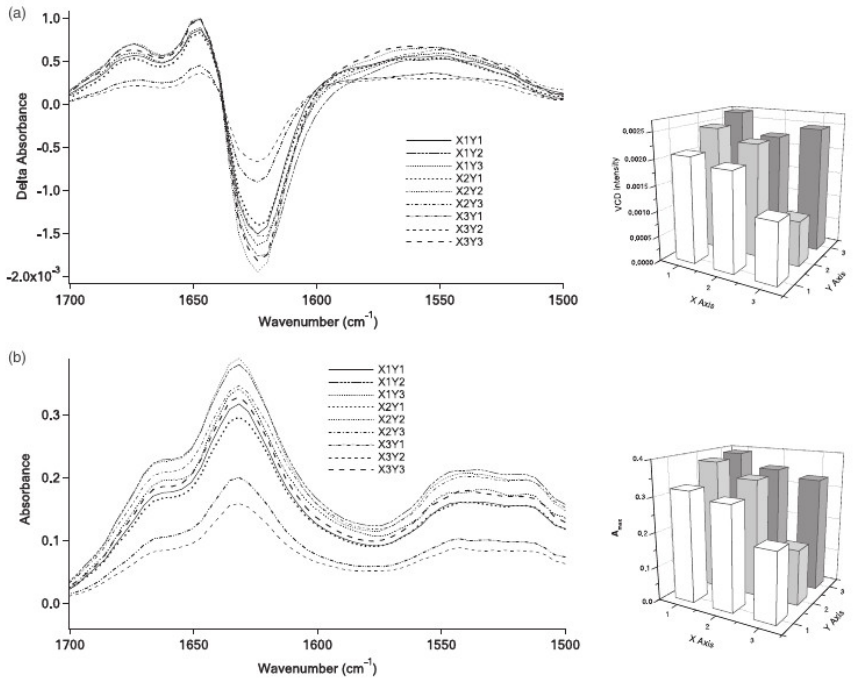

Figure 2.7: (a) VCD and (b) FT-IR spectra of an insulin fibril film at nine non-overlapping 1 mm spots across the film. The intensity of FT-IR absorbance maximum (A_{max}) and VCD intensity difference maximum ($\Delta A_{max} - \Delta A_{min}$) across the amide I and II regions are plotted for each of the nine different spots and shown to the right of the spectra. The FT-IR intensity map reveals different thicknesses of film deposit at different locations of the film. The similarity of the intensity change of VCD and FT-IR indicates that variation of film thickness is the primary reason for the change in intensity over the VCD map. The acquisition time is 20 min for each location.

The achieved resolution is still too low for biological sample microscanning but it should be possible to further enhance the resolution and potentially gain an ability to map biological samples with a sub-millimetre resolution by replacing the $f/1$ lenses with microscopic objectives. This step is complicated by the fact, that the only available microscopic objectives with suitable parameters, Cassegrain reflectors, block the central part of the beam which carries the bulk of the beam intensity and the throughput of the system drops to approximately 15 % of the unmodified VCD system. This results in single point acquisition times of $\sim$1 hour, which is unsuitable for mapping of biological samples. In order to avoid this caveat, modifications to the beam profile of the interferometer have to be designed

and performed in the future, which will open a path for development of high-resolution VCD microscopy systems suitable for studying biological samples.

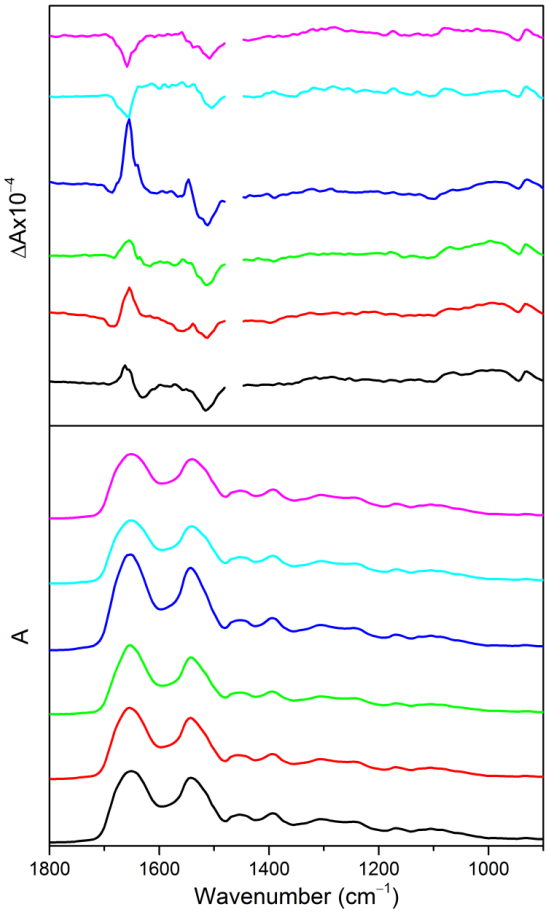

Figure 2.8: Blood samples deposited on CaF_2 slides mapped with 1 mm resolution. Amide I and II bands as well as deoxyribonucleic acid vibrations (PO_2 vibrations located at 1090 cm^{-1} and 1240 cm^{-1}) are visible in the VCD spectra. The acquisition time is 1 hour for each location.

2.1.3 Amide nonplanarity

The amide bond is one of the most important structural features in protein molecules as it chains the individual amino acids together. In many molecules, including proteins, this group can adopt a small degree of nonplanarity [91]. The nonplanarity not only alters the geometry of protein backbone but can also increase basicity of the amide nitrogen and influence biochemical processes. It also introduces an additional degree of freedom for each amino acid residue. In order to investigate this phenomenon, we studied several model compounds from the group of tricyclic spirodilactams ([92], appendix 3, fig. 2.9). These molecules are very rigid and constrain the amide bond to a twisted pyramidal arrangement.

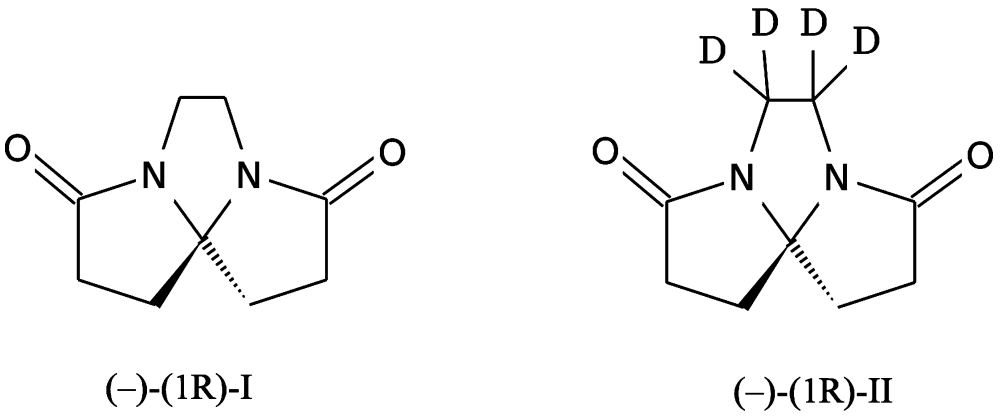

(–)-(1R)-I (–)-(1R)-II

Figure 2.9: Structures of spirodilactam I and II.

The properties of amide bond were probed using ROA and VCD spectroscopies and compared with theoretical calculations using B3LYP functional and 6-311++G** basis set. These comparisons allowed us to perform band-to-band spectral assignment and interpretation (see fig. 2.10). We have also identified influences of the amide linkage nonplanar deformations on the amide I and amide II vibrations. Subsequently, the amide nonplanarity together with amide–amide coupling acting over a several bond distance was identified. Characteristic spectral features for amide nonplanarity detection and absolute conformation assignment were found [92]. The presented data set can also be used as a testing tool for ROA anharmonic corrections within C–H and C–D stretching regions. Since these studies were done on the highly rigid structures, an extension to more flexible molecules should be the next step. Then, our approach will bring a valuable contribution to the understanding of nonplanarity of the amide bond in proteins studied by VOA.

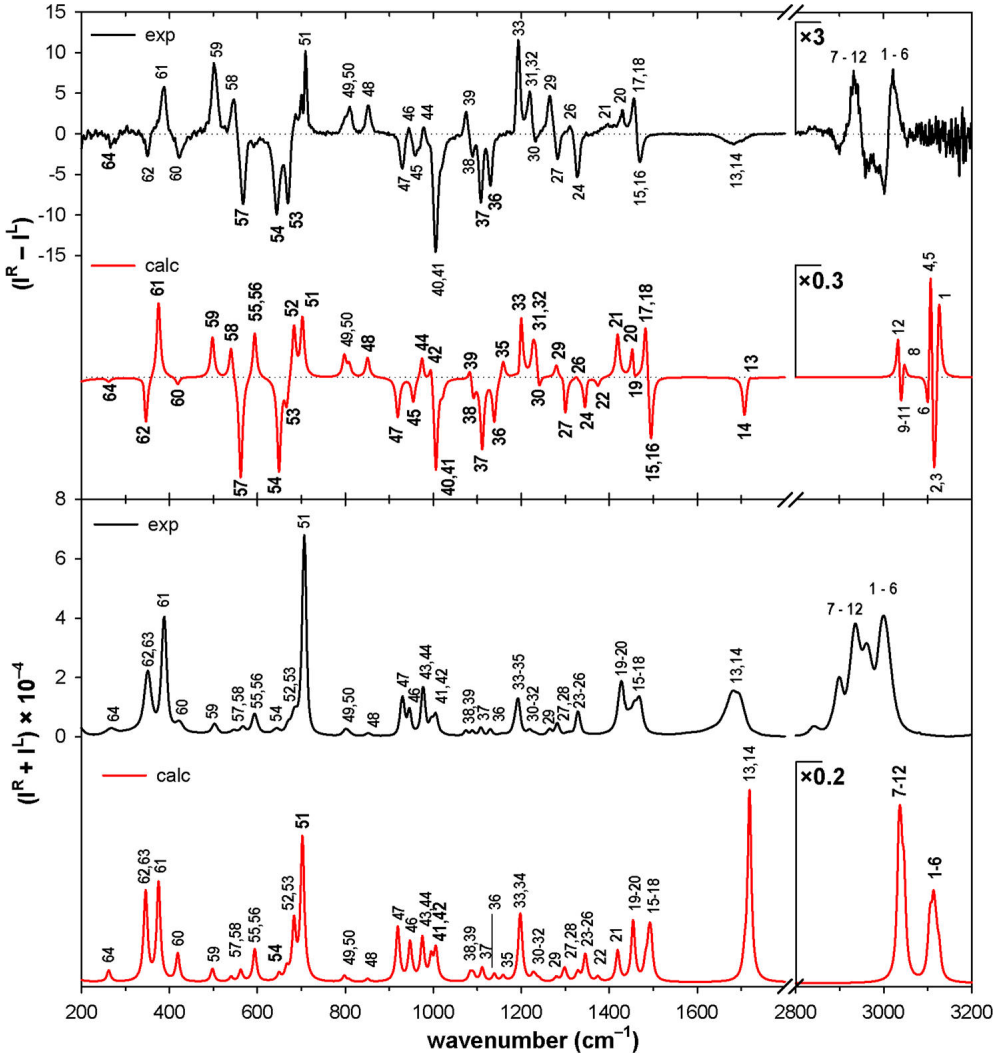

Figure 2.10: Experimental (black) and calculated (red) Raman (bottom) and ROA (top) spectra of the spirodilactam I in water.

2.1.4 Raman spectroscopy of amino acids

As protein constituents, amino acids and their behaviour in aqueous solutions represent important targets in biomolecular spectroscopy, including Raman spectroscopy. Systematically measured amino acid Raman spectra represent valuable testing sets for detailed protein studies (including surface-enhanced Raman scattering (SERS) studies) and can be employed even in the field of practical applications such as analytical chemistry, forensic science or art analysis. Attempts to collect such Raman spectral series of amino acids have been already performed. However, most of the studies used polycrystalline samples only [93] (which are not easily applicable to biomolecular studies in solutions) and also the quality of the spectra was sometimes controversial [94]. Moreover, it has been shown by members of our group that even high-quality Raman measurements of amino acids in solutions, e.g., [95–99] might not be sufficient because Raman spectra of amino acids may exhibit concentration dependence. The dependency of spectral intensities and wavenumbers on sample concentration has been already demonstrated for Pro [100]. It is particularly strong for a solution – glass transition [100]

(glass phase which spectroscopically resembles an "over-saturated" form has been obtained using DCDR). In order to detect possible concentration dependencies, glass forms of the amino acid samples should be therefore included in amino acid measurements.

For these reasons, we have measured Raman spectra of 20 proteinogenic amino acids in solution, glass phase (as DCDR samples) and crystalline forms in the wide spectral range of 200–3200 cm^{-1} ([101], appendix 4). Obtaining amino acids in the glass phase is not an easy task because amino acids tend to form quasi-crystals or crystals upon formation of the DCDR ring (fig. 2.11). Thus, experimental conditions for diluting each amino acid had to be adjusted to avoid formation of sub-micro crystals.

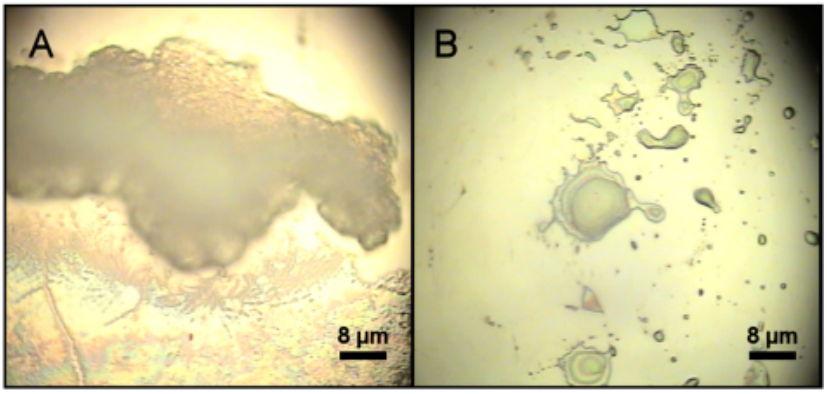

Figure 2.11: Photos of alanine forming a microcrystalline phase upon formation of a DCDR ring (A) and a true drop coating – glass phase – of the same amino acid at lower concentration (B) when the former DCDR ring disintegrates into small stable coated regions.

The spectral differences between the Raman spectra of the crystalline forms, glass phases and aqueous solutions of the amino acids have been described in Pazderka *et al.* ([101], appendix 4). A strong influence of sample density and organization of the hydration shell has been observed for several amino acids. The most prominent changes have been found for Ser and Thr where hydration shell strongly influences a number of vibrations (fig. 2.12). In contrast, amino acids with aromatic side chains have only a small sensitivity to the form of the sample (fig. 2.13). DCDR spectra of a majority of the amino acids represent an intermediate between the solution and crystalline forms. Our reference set of Raman spectra is useful for revealing discrepancies between SERS and solid/solution spectra of the amino acids. It is due to the fact that concentrations of amino acids measured on SERS-active substrates, which are becoming increasingly popular and also commercially available, are very similar to those used for DCDR spectroscopy. Thus, DCDR spectra can be mistaken for SERS spectra if the solution sample is dried by the "coffee ring effect" on a solid SERS substrate. This is probably the case of the SERS measurement of a set of 19 amino acids in the work of Botta *et al.* [102]. We have also found out that some previously published Raman spectra of polycrystalline samples resemble glassy state rather than crystalline spectra [103]. Therefore, our study clearly demonstrated that, when measuring Raman spectra of amino acids, particular attention has to be paid to the experimental conditions.

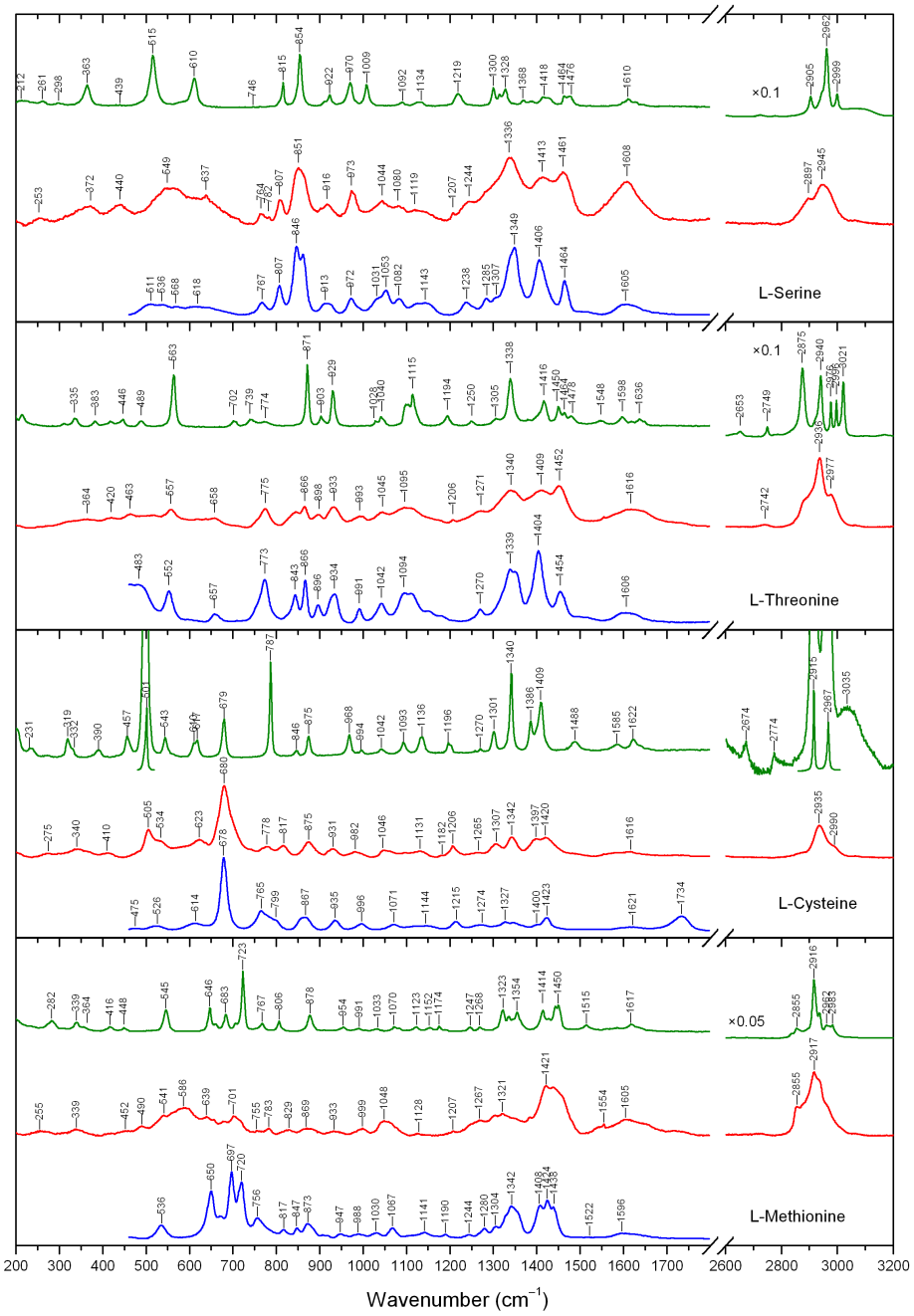

Figure 2.12: Raman spectra of hydroxyl amino acids Ser and Thr and sulphur-containing Cys and Met in aqueous solutions (lowest blue curves), in glass forms (middle red curves) and in crystalline forms (upper green curves).

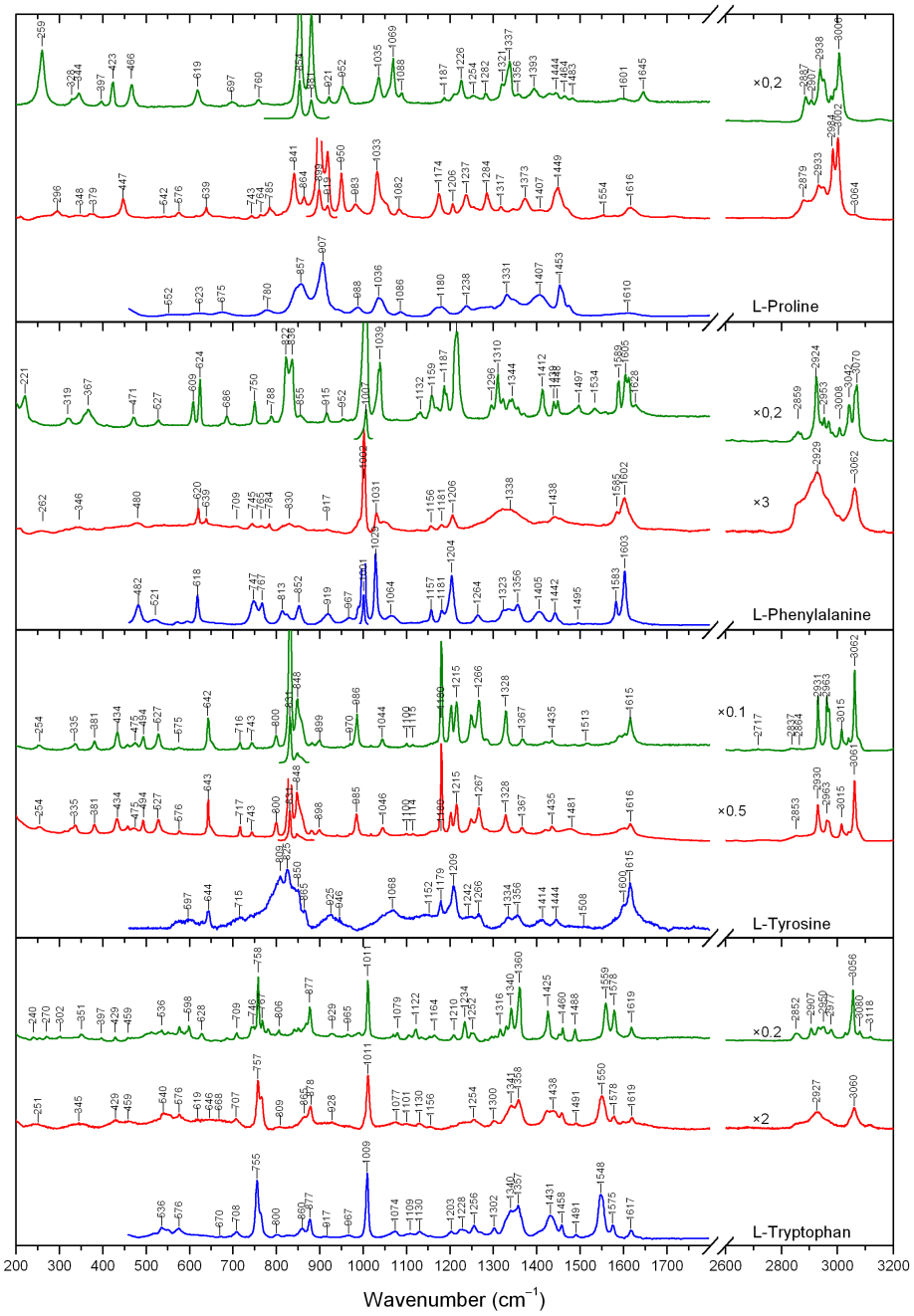

Figure 2.13: Raman spectra of cyclic and aromatic amino acids Pro, Phe, Tyr and Trp in aqueous solutions (lowest blue curves), in glass forms (middle red curves) and in crystalline forms (upper green curves).

2.2 Protein dynamics

2.2.1 Two-dimensional correlation analysis

2DCoS is an excellent tool for studying protein dynamics due to its ability to reveal order of spectral changes and their synchronicity. It allows us to analyse in

detail effects of thermal denaturation which is a common tool for protein dynamics studies.

Data treatment protocol

Utilization of 2DCoS for VOA measurements is still quite novel [56, 104, 105]. One major drawback is a necessity of a complex data pretreatment [106] which is required particularly due to a low SNR and background fluctuations. Because no proper data treatment protocols have been reported previously, we have focused on creating a reproducible and well-established protocol for such pretreatment ([107], appendix 5, fig. 2.14). As a first step, we apply a Fourier filter in order to suppress a quasi-periodic high-frequency signal in the low wavenumber region. This signal is mainly caused by a laser interference on cell walls and can be suppressed using thin-wall cells or by masking the cell space in order to remove non-paraxial beams (if no such signal is present, this step can be omitted). As a next step, VOA signal of the solvent-filled cell (preferably the identical cell) is subtracted. This subtraction should be performed even if the solvent is non-chiral because the solvent spectrum is affected by the same baseline distortions from the experimental setup as the sample spectrum [8]. Since the "solvent" spectrum is usually simple, it can be easily fitted with a spline curve (which is used in order not to decrease SNR).

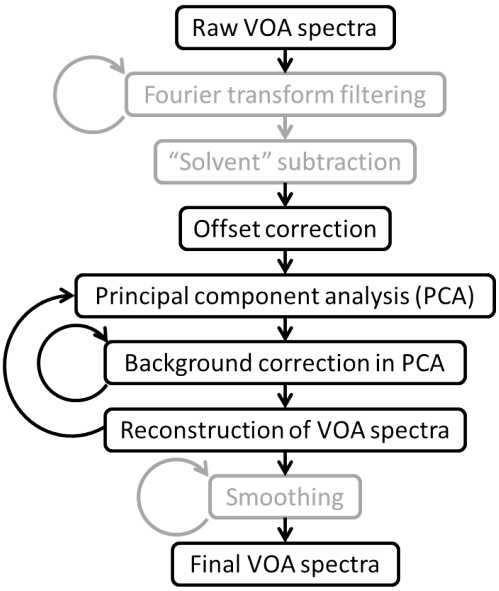

Figure 2.14: The scheme depicts the proposed data treatment of VOA spectra. Gray parts of the scheme are optional and depend on quality of the data as well as on stability of the VOA device.

With these steps applied to each individual spectrum, we can proceed with treating the series as a whole. The corrections performed on individual spectra bring inconsistencies which would be enhanced in 2DCoS spectra. Therefore, the best approach is to employ a multivariate statistics (for example PCA) to decompose the data into principal components and perform the corrections directly on these components. Background variations are usually comprised of broad bands and/or slope variations of the baseline, which can be easily identified and removed

from individual subspectra using splines. This step is arbitrary and depends on user's experience and skills. However, it is much more consistent than an individual treatment of each spectra. After treating all the significant subspectra, the spectral set can be reconstructed again. This also allows further reducing the noise because only significant subspectra are included in the reconstruction of the data. This procedure enhances the quality of 2DCoS spectra significantly as can be seen in fig. 2.15.

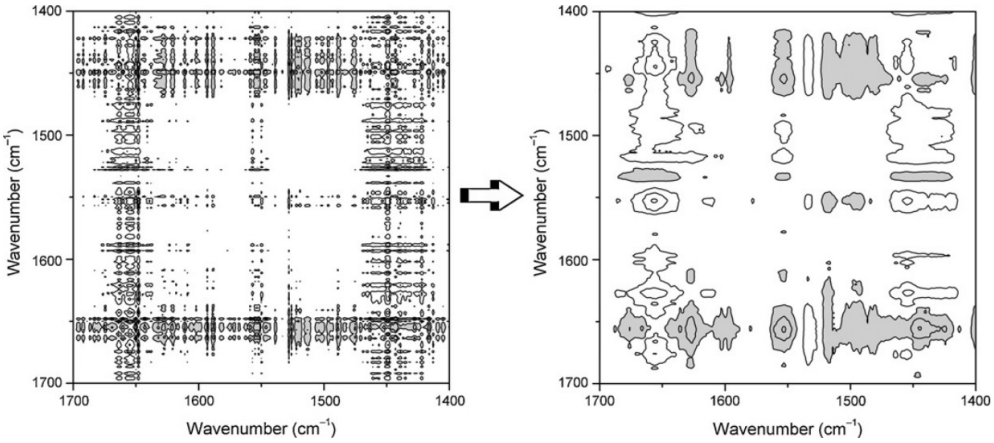

Figure 2.15: The figure on the left depicts 2DCoS asynchronous plot calculated from original raw VOA spectra of protein thermal denaturation. The figure on the right represents resulting asynchronous 2DCoS of the VOA data with performed PCA pretreatment.

Extension of the rules to bisignate spectra

In order to understand the results of 2DCoS applied to VOA spectra, an extension of regular "Noda rules" to bisignate spectra has to be performed. Only one such attempt has yet been reported [106]. However, only simple model spectra were used for demonstration of the band sign in ROA spectra and no attention was given to spectral shapes. Spectral bands were simulated using their intensity and no spectral bandwidth was taken into account. Thus, only basic rules for 2DCoS were verified but the study could not cover all spectral phenomena (e.g., bandwidth changes, spectral shifts and their combinations) that are present in VOA spectra, which contain both positive and negative bands. Following our previous work [108] we have focused on a detailed simulation of spectral patterns using Gaussian and Lorentzian band shapes in bisignate spectra ([107], appendix 5). Since 2DCoS examines only relative directions of the changes and not the absolute values, the Noda rules can be directly applied to VOA spectra. The only difference in the rules is for synchronous spectrum, where the rules are reversed for peaks of the opposite sign. This phenomenon is shown in fig. 2.16, where A and B represent a peak broadening for vibrational spectra and VOA spectra, respectively. In general, the patterns are similar to those found in conventional vibrational spectra. The patterns in ROA spectra usually become more complex due to a close proximity of two peaks forming a couplet. Individual patterns, known from vibrational spectroscopy, are still observable but they sometimes blend together forming new, slightly different patterns.

This extension allows us to further investigate dynamic processes in proteins (i.e., unfolding, denaturation, ligand binding).

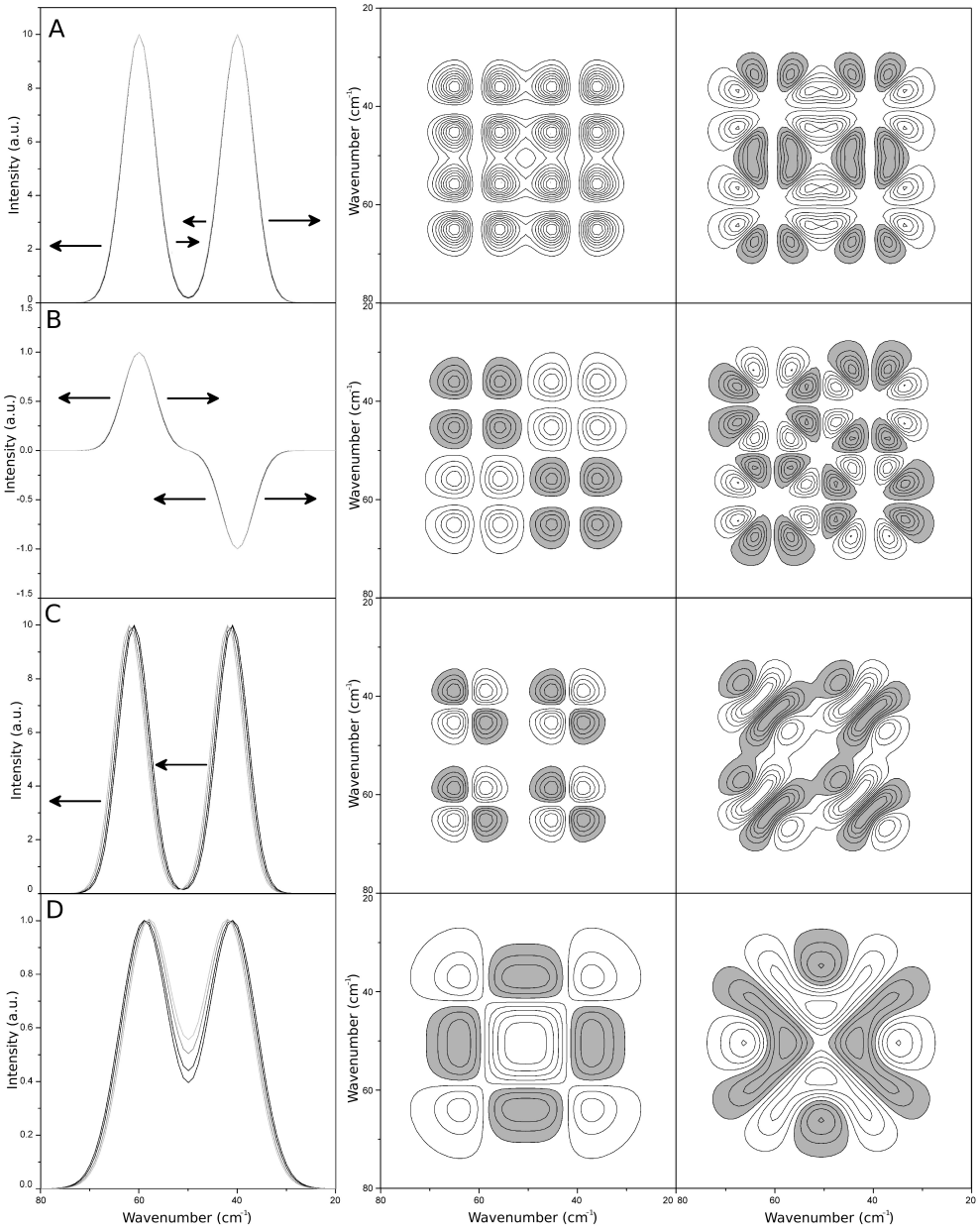

Figure 2.16: Comparison of behaviour of classical (monosignate) and VOA spectra of Gaussian shapes together with their synchronous and asynchronous 2DCoS. Eleven spectra were simulated in all cases. (A) Two classical peaks broadening by 5 %, (B) VOA couplet of opposite signs broadening by 5 %, (C) two classical bands moving jointly in the same direction by 1 % and (D) two peaks moving against each other by 1 %.

Hetero two-dimensional correlation spectroscopy

2DCoS can be generalised to correlate experimental spectra obtained with different probes, different perturbations or even from different samples [68]. There are three types of hetero-correlation analysis: (i) hetero-spectral correlation, where

two different spectral probes are used [109, 110]; (ii) hetero-perturbation correlation, where two different perturbations are used [111]; (iii) hetero-sample, where two different samples serve as an input for 2DCoS analysis [68]. Another, purely mathematical, version of cross-spectral correlation called concatenated 2DCoS was proposed by L. Zhang *et al.* [112]. This method applies mirror concatenation on spectral data set along the perturbation axis. This increases the sensitivity of 2DCoS to irreversible changes [112, 113]. It is also possible to apply the 2DCoS repeatedly on properly rescaled data. This method, called double 2DCoS, generates correlation spectra with higher selectivity and spectral resolution [114–116].

Spectral patterns and rules in hetero-sample correlation were investigated previously, but simulated spectra had very different spectral patterns [117]. We have focused on correlation of two samples having very similar spectral pattern as we were interested in studies of closely related protein species. In order to understand and interpret the results of hetero-sample correlation of such systems we first analysed correlation of simulated dataset (appendix 6, fig. 2.17). The observed spectral patterns are similar to those predicted by Noda, thus regular Noda rules are applicable in this case.

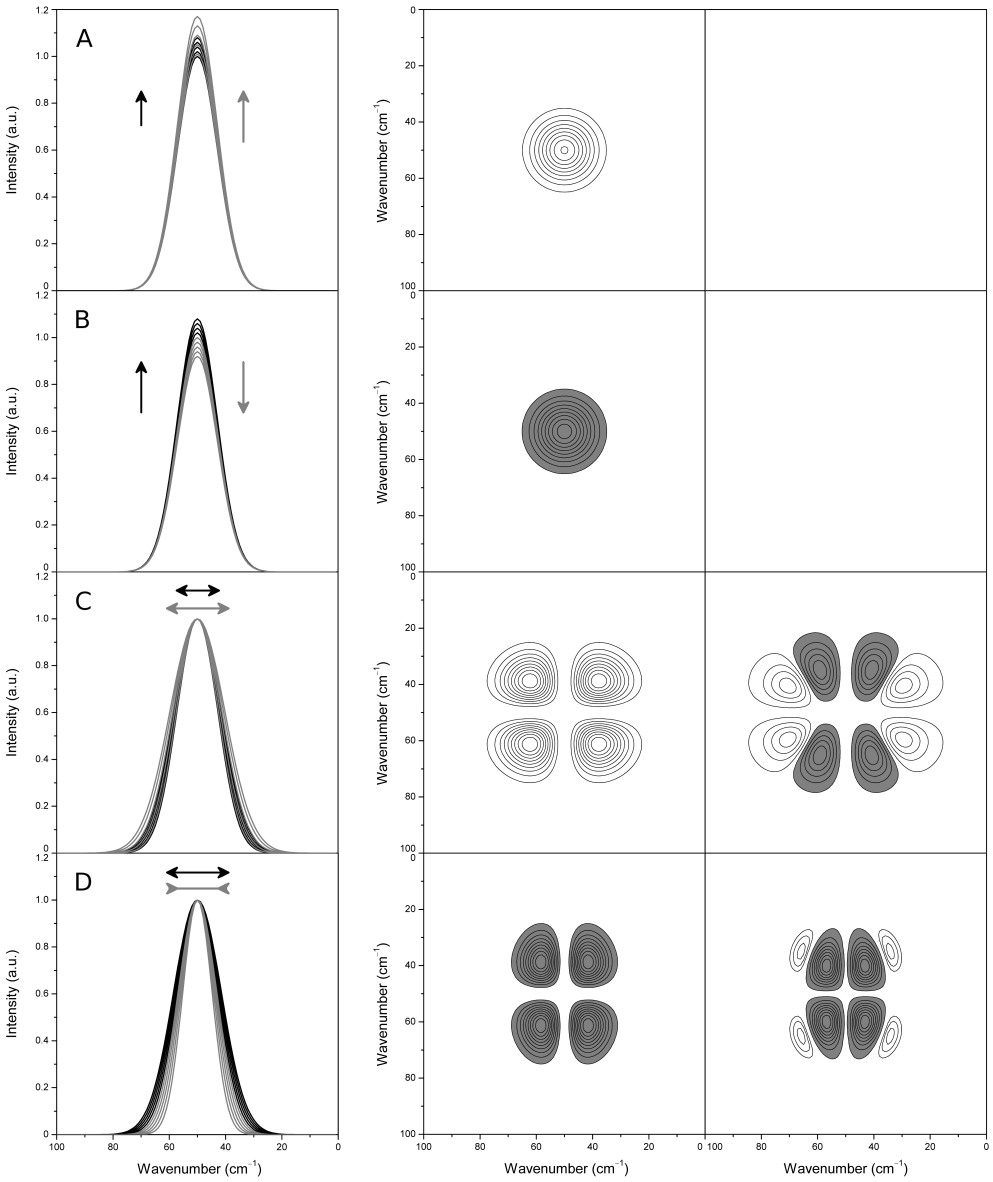

Figure 2.17: The simulated process of intensity changes in spectra of Gaussian shapes together with their hetero-sample synchronous and asynchronous 2DCoS spectra. Ten spectra were simulated in all cases. (A) Two bands are increasing with different rates, (B) the first band is increasing while the latter is decreasing with the same rate, (C) two bands are broadening with different rates, and (D) the bandwidth of the first band increases and the second one decreases with the same rate. (Shaded areas indicate negative correlation intensity.)

2.2.2 Protein oligomerization studied by two-dimensional correlation spectroscopy

Human haptoglobin (Hp) is a protein from a blood plasma belonging to a group of serum α_2-glycoproteins. Hp plays an important role in an immune system and in a response to shock conditions. It participates in a hemoglobin transport [118] and prevents its degradation in kidneys [119]. Hp also has a chaperone-like activity in preventing thermally induced protein aggregation [120] and it has

been shown that it undergoes a significant conformational transition upon heating [120]. Hp is a tetramer with two light α-chains and two heavy β-chains [119, 120], covalently bonded by disulphide bridges. In humans, it exists in three phenotypes which differ in the length of the α-chain: (i) Hp 1-1 having the α-chain with 83 amino acids in both subunits; (ii) Hp 2-2 with the α-chain of 142 amino acids in both subunits; (iii) Hp 1-2 which has one light and one heavy α-chain [121, 122]. These phenotypes have different hemoglobin affinities [123].

Different models characterizing multimeric state of Hp phenotypes have been already proposed [122]. However, the reason for prevalence of Hp2 form remains unclear. In order to better understand different haptoglobin phenotypes in human populations, we have examined structural and dynamical behaviour of the Hp 1-1 and Hp 2-2 phenotypes by IR spectroscopy using 2DCoS. Both phenotypes were studied in the range between 5 and 80 ℃ with 5 ℃ steps. 2DCoS spectroscopy was then applied to the experimental spectra, both in regular variant and in hetero variants (appendix 6). Regular 2DCoS (fig. 2.18) identified several differences between the phenotypes – the most important being a difference in a formation of the intermolecular β-sheets. More detailed differentiation was not possible. Application of hetero-sample 2DCoS on the spectra of Hp 1-1 and Hp 2-2 revealed that the synchronous changes are almost identical (fig. 2.19 – A), suggesting that the common parts of both phenotypes have the same thermal dynamics. Concatenated 2DCoS allowed us to study the rate constants of the individual changes for both phenotypes (fig. 2.19 – B). Different rates of the changes indicate that the presence of elongated α-chain in Hp 2–2 (having extra 59 amino acids) makes this phenotype more resistant to the heat-shock. These results were further confirmed by application of double 2DCoS spectroscopy (fig. 2.19 – C).

In addition, structural and dynamical behaviour of both Hp phenotypes has been studied by Raman spectroscopy. PCA and 2DCoS (in regular and hetero-sample variant) have been applied to Raman spectra but proper data analysis has yet to be performed. Preliminary PCA and 2DCoS analysis indicates identical behaviour of the protein core in both phenotypes and increased stability of Hp 2-2 (fig. 2.20) which is in agreement with the results of FT-IR data analysis.

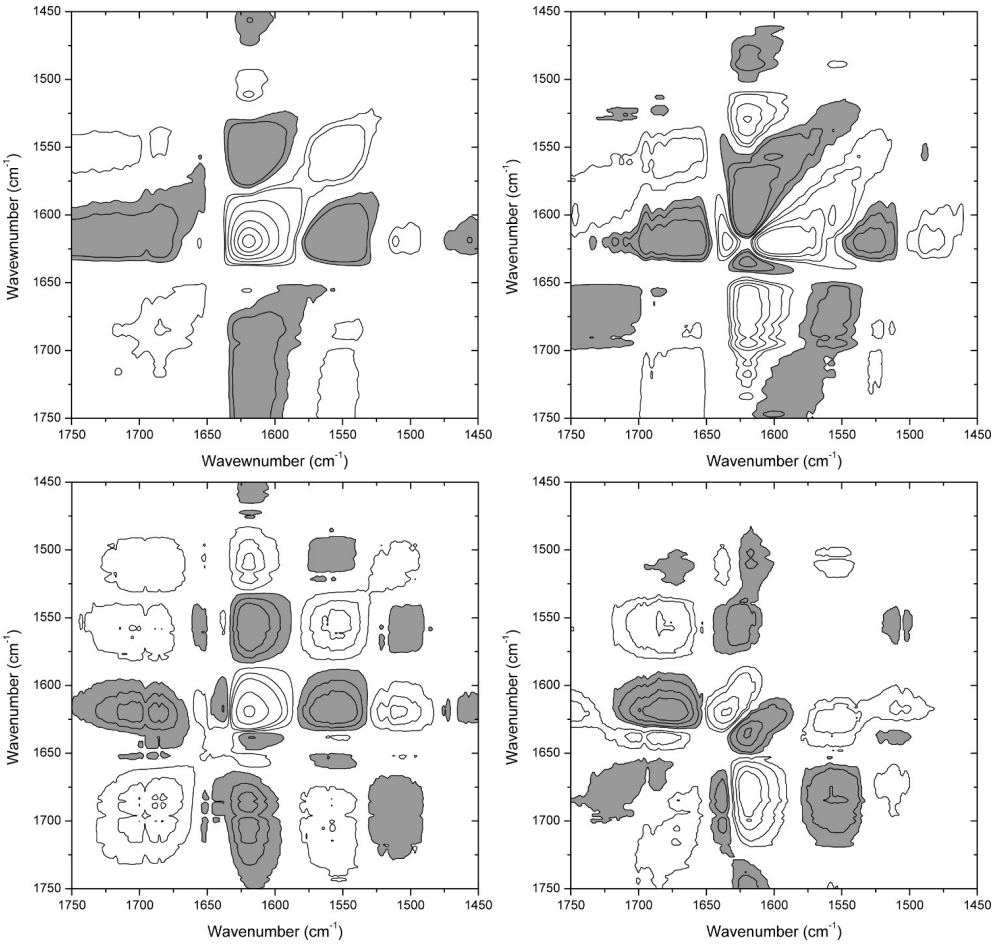

Figure 2.18: 2DCoS of thermal dependencies of infrared spectra of Hp 1-1 (upper row) and Hp 2-2 phenotypes (bottom row). The left column depicts synchronous and the right one asynchronous part of 2DCoS. (Shaded areas indicate negative correlation intensity.)

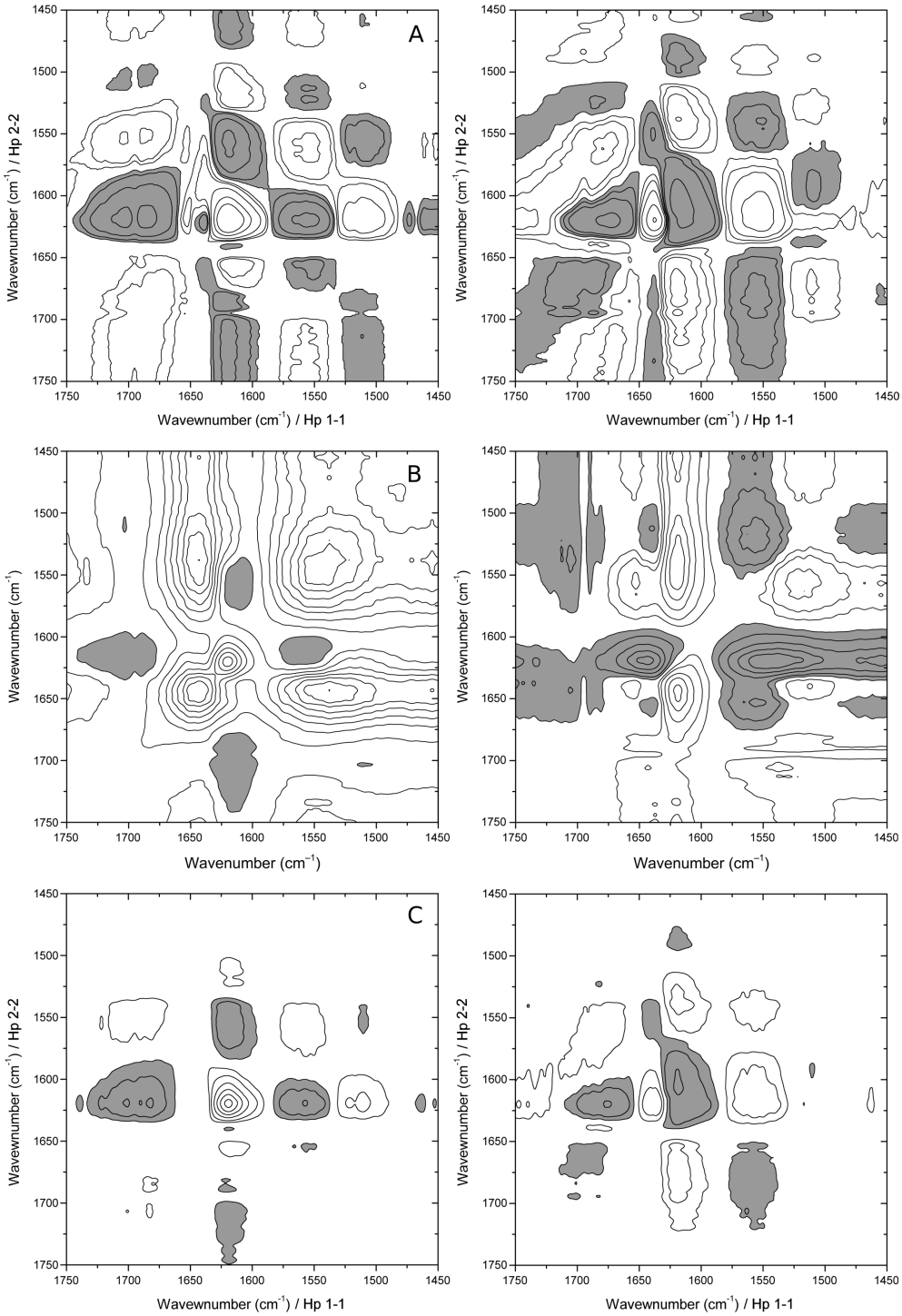

Figure 2.19: The thermal dependencies of infrared spectra of Hp 1-1 and Hp 2-2 phenotypes analysed by hetero-sample 2DCoS (A), concatenated 2DCoS (B), and double 2DCoS with quadrature projected data (C). The left column depicts a synchronous part and the right one an asynchronous part of the 2DCoS. (A) Hetero-sample correlation of Hp 1-1 vs. Hp 2-2, (B) concatenated 2DCoS constructed by the conjunction of Hp 1-1 and reversed Hp 2-2 data (C) double 2DCoS. (Shaded areas represent a negative correlation intensity.)

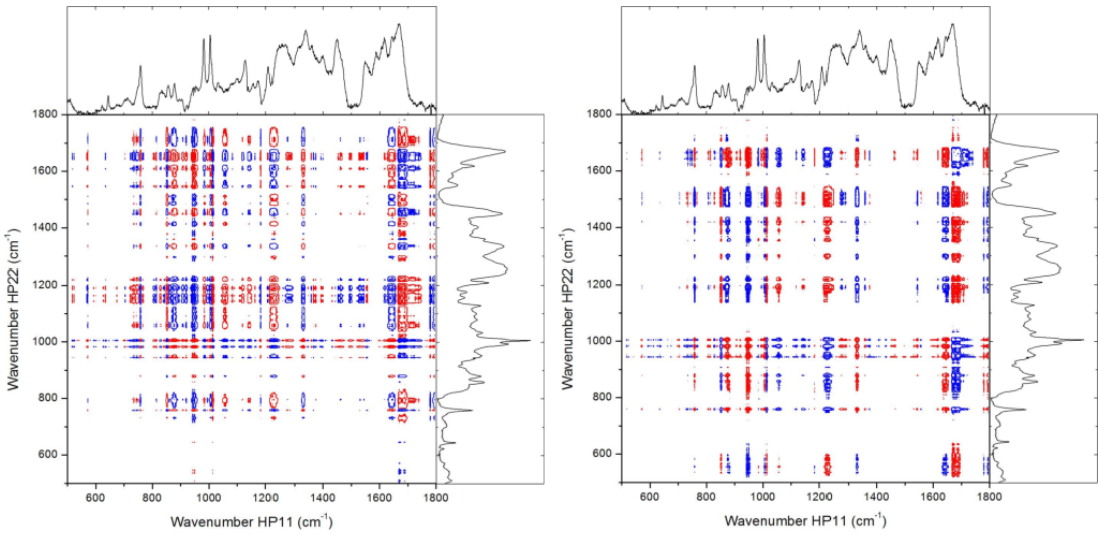

Figure 2.20: The thermal dependencies of Raman spectra of Hp 1-1 and Hp 2-2 phenotypes analysed by hetero-sample 2DCoS. (Red colour indicates positive peaks and blue indicates negative peaks.

2.2.3 Influence of ligand binding on molecular stability and dynamics

Interactions between proteins and ligands play an important role in many biological processes. Binding of the ligand typically changes protein structure and can therefore influence the dynamics and stability of the protein. We have investigated the effect of ligand binding on protein stability and dynamics using the α_1-acid glycoprotein (AGP) – a blood plasma glycoprotein from lipocalin protein family. AGP was studied using a combination of Raman spectroscopy and computer modelling ([124], appendix 7) and the effect of ligand binding on protein structure was determined by combining *in vivo* and *in silico* methods.

Raman spectra of AGP in interaction with various ligands revealed comparable spectral differences which correspond to expected similar structural changes. However, the intensities of the changes for particular ligands differed and corresponded to the already published binding energies [125] and those obtained by computer modelling.

For investigation of the effect of ligand binding on protein stability, we have used the strongest binding ligand – warfarin. The protein stability has been studied by Raman spectroscopy and subsequent PCA analysis of thermally induced denaturation of the free protein and the protein–ligand complex has been performed. Individual structural changes during the process of denaturation have been identified using PCA subspectra and corresponding coefficients. The coefficients of the second subspectrum have been used for determination of protein denaturation temperature (fig. 2.21-B). The coefficients of the third subspectrum show that the melting of AGP is connected with a transition of α-helices to β-turn structure accompanied by structural changes in aromatic amino acids side chains (fig. 2.21-C). Binding of the ligand increases the denaturation temperature and stabilises the protein–ligand complex. These results have been also supported by computer modelling as the resulting experimental and calculated binding energies are in a good agreement [124].

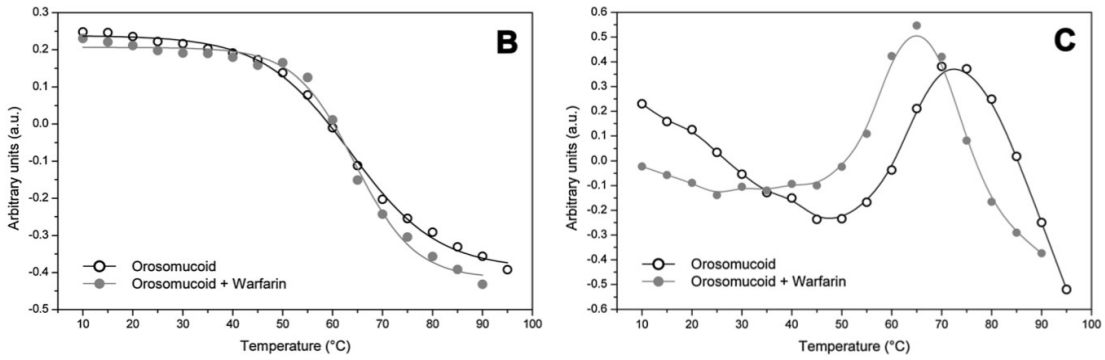

Figure 2.21: (B) The coefficients of the second subspectra V_{i2} of PCA of thermal denaturation of AGP in the native state and with warfarin as a ligand. The coefficients were fitted by a sigmoidal function. (C) The coefficients of the third subspectra V_{i3} of PCA of the thermal denaturation of AGP in the native state and with warfarin as a ligand. The values were fitted by B-splines.

2.2.4 Protein fibrillation

As has been already demonstrated, VCD is an excellent tool for studies of protein fibrils as the VCD signal of the fibrils is increased by over an order of magnitude compared to the spectrum of an isolated protein [15]. Despite an intense research and modelling attempts, an origin of this enhancement is still unclear [126, 127].

Experimental VCD spectra of fibrils in H_2O typically exhibit a complex five-band pattern, which covers both amide I and amide II regions. In order to distinguish bands arising from the amide I and amide II vibrations, we have measured VCD spectra of fibrils from hen egg white lysozyme (HEWL) and human insulin (HI) grown in H_2O/D_2O at different pH/pD values (i.e., above and below transition point for reversed chirality [87]). Direct comparison of fibrils grown in H_2O and D_2O allows us to separate vibrations arising from amide I region. The overall 5-band pattern is reduced to only 3 or 4 bands in amide I region ([128], appendix 8) due to downshifting of the amide II region in deuterated samples. Further inspection of the deuterated spectra also shows that the amide I bands do not exhibit an intensity bias compared to a positive/negative bias in the spectra of fibrils grown in H_2O (fig. 2.22). These findings justify the theoretical calculations of the fibril VCD enhancement based on a coupled-oscillator model [126] and should serve as valuable testing data for further modelling attempts.

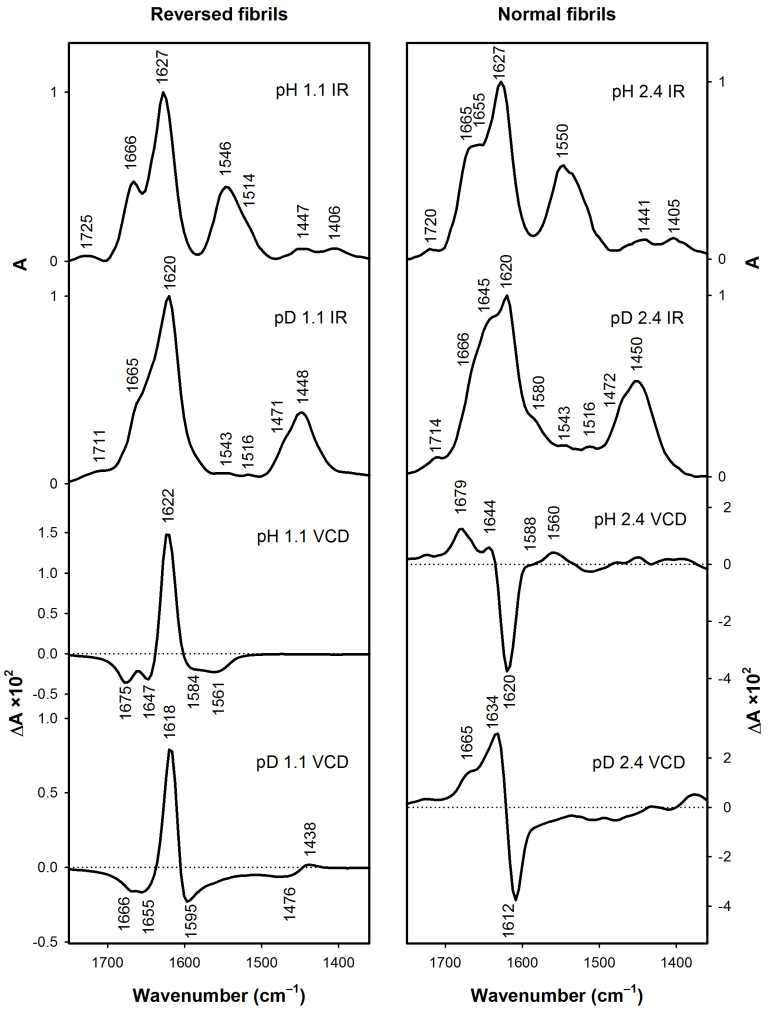

Figure 2.22: VCD and FT-IR spectra of HEWL fibrils grown in H_2O and D_2O (samples prepared under the same conditions: pH/pD adjusted to 1.1 and 2.4, samples incubated at 65 ℃ for 3 days).

Conclusion

The goal of this dissertation thesis was to improve experimental setup and data processing for vibrational and VOA spectroscopies allowing novel approaches in studies of protein structure and dynamics. All these improvements have been tested and their feasibility has been verified using selected protein systems.

- Microsampling stage for VCD measurements has been developed and built. We have achieved a spatial resolution of 1 mm with a throughput of 50% and verified that the setup is artefact-free. The feasibility of this setup has been verified by measuring several samples of HI fibrils. Preliminary measurements of blood samples, animal cells and tissue samples with fibril plaques have been performed.

- We have investigated processes connected with protein fibrillation using methods of VOA and showed that they are a useful tool for such studies. We have measured VCD spectra of protein fibrils grown in H_2O/D_2O and identified signals arising from amide I vibrations. This identification and band separation is important for calculations of fibril VCD spectra.

- A comprehensive set of amino acid Raman spectra measured in solution, glass, and crystalline phase was obtained. Spectral dependencies on concentration and phase were identified and discussed. This set may serve as a valuable testing data set for various fields of science (e.g., SERS substrate research, forensic science or astrobiological in situ planetary research).

- We have demonstrated usefulness of intensity calibration and tested the comparability of data measured on three different instruments and using several configurations. This approach is easy to incorporate into regular ROA measurements and improves the overall quality of the ROA spectra. Improved comparison of theoretical and experimental data has also been demonstrated.

- We have extended the current understanding of 2DCoS to the methods exhibiting bisignate spectra, with special focus on VOA. The most common spectral shapes present in VOA have been modelled and 2DCoS spectra have been calculated and analysed. We have verified that Noda rules are, with a small modification, applicable to 2DCoS spectra computed from bisignate spectra. We have also established a procedure for spectral data pretreatment which results in high-quality and reproducible 2DCoS spectra.

- Dynamical behaviour of two Hp phenotypes has been studied using a combination of vibrational spectroscopy and hetero-sample 2DCoS. Hetero-sample 2DCoS has been used to identify identical behaviour of common parts of both phenotypes. The results of concatenated 2DCoS have shown that a prolongation of the α-chain of Hp 2-2 is important for its increased thermal stability.

- Amide nonplanarity has been investigated by several spectroscopic methods using model dilactams having two nonplanar amide groups. We have successfully identified chiroptical response of nonplanar amide group in rigid

environment. The identified spectral features can be used for amide non-planarity detection and absolute conformation determination.

- Interaction of AGP with different ligands has been investigated using Raman spectroscopy. Dynamics of the resulting complex has been studied by thermal denaturation and PCA which allowed us to calculate the denaturation temperature. Protein stabilisation has been then confirmed by computer modelling.

Bibliography

[1] B. Alberts, *Essential Cell Biology*. Garland Science, 1998.

[2] P. V. Baranov, R. F. Gesteland, and J. F. Atkins, "Recoding: translational bifurcations in gene expression," *Gene*, vol. 286, no. 2, pp. 187–201, 2002.

[3] D. Whitford, *Proteins: Structure and Function*. Chichester: Wiley, 2005.

[4] G. Ramachandran, C. Ramakrishnan, and V. Sasisekharan, "Stereochemistry of polypeptide chain configurations," *Journal of Molecular Biology*, vol. 7, no. 1, pp. 95–99, 1963.

[5] P. Tompa, *Strucutre and Function of Intrinsically Disordered Proteins*. Boca Raton: Chapman and Hall/CRC, 2009.

[6] M. Gerstein, A. M. Lesk, and C. Chothia, "Structural mechanisms for domain movements in proteins," *Biochemistry*, vol. 33, no. 22, pp. 6739–6749, 1994.

[7] S. C. L. Kamerlin and A. Warshel, "At the dawn of the 21st century: Is dynamics the missing link for understanding enzyme catalysis?" *Proteins*, vol. 78, no. 6, pp. 1339–75, 2010.

[8] J. Kapitán, V. Baumruk, H. Hulačová, and P. Maloň, "Raman optical activity of the hinge peptide," *Vibrational Spectroscopy*, vol. 42, no. 1, pp. 88–92, 2006.

[9] V. Kopecký Jr., R. Ettrich, K. Hofbauerová, and V. Baumruk, "Structure of human α_1-acid glycoprotein and its high-affinity binding site," *Biochemical and Biophysical Research Communications*, vol. 300, no. 1, pp. 41–46, 2003.

[10] A. Fersht, *Structure and Mechanism in Protein Science*. New York: W. H. Freeman and Company, 1998.

[11] C. M. Dobson, "Protein folding and misfolding," *Nature*, vol. 426, no. 6968, pp. 884–890, 2003.

[12] D. R. Booth, M. Sunde, V. Bellotti, C. V. Robinson, W. L. Hutchinson, P. E. Fraser, P. N. Hawkins, C. M. Dobson, S. E. Radford, C. C. F. Blake, and M. B. Pepys, "Instability, unfolding and aggregation of human lysozyme variants underlying amyloid fibrillogenesis," *Nature*, vol. 385, pp. 787–793, 1997.

[13] H. A. Havel, *Spectroscopic Methods for Determining Protein Structure in Solution*. Wiley-VCH, 1996.

[14] A. Barth, "The infrared absorption of amino acid side chains," *Progress in Biophysics and Molecular Biology*, vol. 74, no. 3-5, pp. 141–173, 2000.

[15] L. A. Nafie, *Vibrational Optical Activity: Principles and Applications*. Chichester, UK: Wiley, 2011.

[16] H. Fabian and W. Mäntele, "Infrared spectroscopy of proteins," in *Handbook of Vibrational Spectroscopy*, J. M. Chalmers, Ed., Chichester, UK: Wiley, 2006.

[17] H. Yang, S. Yang, J. Kong, A. Dong, and S. Yu, "Obtaining information about protein secondary structures in aqueous solution using Fourier transform IR spectroscopy," *Nature Protocols*, vol. 10, no. 3, pp. 382–396, 2015.

[18] S. Krimm and J. Bandekar, "Vibrational spectroscopy and conformation of peptides, polypeptides, and proteins," *Advances in Protein Chemistry*, vol. 38, pp. 181–364, 1986.

[19] A. Barth, "Infrared spectroscopy of proteins," *Biochimica et Biophysica Acta – Bioenergetics*, vol. 1767, no. 9, pp. 1073–1101, 2007.

[20] M. Diem, *Introduction to Modern Vibrational Spectroscopy*. John Wiley & Sons, 1993, p. 285.

[21] A. Barth and C. Zscherp, "What vibrations tell us about proteins," *Quarterly Reviews of Biophysics*, vol. 35, no. 4, pp. 369–430, 2002.

[22] A. Dong, P. Huang, and W. Caughey, "Protein secondary structures in water from second-derivative amide I infrared spectra," *Biochemistry*, vol. 29, no. 13, pp. 3303–3308, 1990.

[23] K. Rahmelow and W. Hübner, "Secondary structure determination of proteins in aqueous solution by infrared spectroscopy: a comparison of multivariate data analysis methods," *Analytical Biochemistry*, vol. 241, no. 1, pp. 5–13, 1996.

[24] F. Dousseau, M. Therrien, and M. Pézolet, "On the spectral subtraction of water from the FT-IR spectra of aqueous solutions of proteins," *Applied Spectroscopy*, vol. 43, no. 3, pp. 538–542, 1989.

[25] V. Baumruk, P. Pancoska, and T. A. Keiderling, "Predictions of secondary structure using statistical analyses of electronic and vibrational circular dichroism and Fourier transform infrared spectra of proteins in H_2O," *Journal of Molecular Biology*, vol. 259, no. 4, pp. 774–791, 1996.

[26] C. Jung, "Insight into protein structure and protein-ligand recognition by Fourier transform infrared spectroscopy," *Journal of Molecular Recognition*, vol. 13, no. 6, pp. 325–351, 2000.

[27] K. Griebenow and A. M. Klibanov, *Proceedings of the National Academy of Sciences of the United States of America*, vol. 92, no. 24, pp. 10 969–10 976, 1995.

[28] G. G. Glenner, E. D. Eanes, H. A. Bladen, R. P. Linke, and J. D. Termine, "β-pleated sheet fibrils a comparison of native amyloid with synthetic protein fibrils," *Journal of Histochemistry & Cytochemistry*, vol. 22, no. 12, pp. 1141–1158, 1974.

[29] P. R. Carey, *Biochemical Applications of Raman and Resonance Raman SPectroscopies*. Academic Press, 1982, p. 262.

[30] P. R. Carey, "Raman spectroscopy, the sleeping giant in structural biology, awakes," *Journal of Biological Chemistry*, vol. 274, no. 38, pp. 26 625–8, 1999.

[31] T. Miura and G. J. Thomas, "Raman spectroscopy of proteins and their assemblies," in *Proteins: Strucutre, Function, and Engineering*, B. B. Biswas and S. Roy, Eds. Springer, Boston, MA, 1995, pp. 55–99.

[32] M. N. Siamwiza, R. C. Lord, M. C. Chen, T. Takamatsu, I. Harada, H. Matsuura, and T. Shimanouchi, "Interpretation of the doublet at 850 and 830 cm^{-1} in the Raman Spectra of tyrosyl residues in proteins and certain model compounds," *Biochemistry*, vol. 14, no. 22, pp. 4870–4876, 1975.

[33] T. Miura, H. Takeuchi, and I. Harada, "Characterization of individual tryptophan side chains in proteins using Raman spectroscopy and hydrogen-deuterium exchange kinetics," *Biochemistry*, 1988.

[34] T. Miura, H. Takeuchi, and I. Harada, "Raman spectroscopic characterization of Tryptophan side chains in lysozyme bound to inhibitors: Role of the hydrophobic box in the enzymatic function," *Biochemistry*, vol. 30, no. 24, pp. 6074–6080, 1991.

[35] T. Kitagawa and S. Hirota, "Raman spectroscopy of proteins," in *Handbook of Vibrational Spectroscopy*, J. M. Chalmers, Ed., Chichester, UK: Wiley, 2006.

[36] H. E. Van Wart and H. A. Scheraga, "Raman spectra of cystine-related disulfides. Effect of rotational isomerism about carbon-sulfur bonds on sulfur-sulfur stretching frequencies," *The Journal of Physical Chemistry*, vol. 80, no. 16, pp. 1812–1823, 1976.

[37] H. M. Li and G. J. Thomas, "Cysteine conformation and sulfhydryl interactions in proteins and viruses. 1. correlation of the Raman S–H band with hydrogen-bonding and intramolecular geometry in model compounds," *Journal of the American Chemical Society*, vol. 113, no. 2, pp. 456–462, 1991.

[38] G. J. Thomas, "New structural insights from Raman spectroscopy of proteins and their assemblies," *Biopolymers*, vol. 67, no. 4–5, pp. 214–225, 2002.

[39] D. Zhang, Y. Xie, M. F. Mrozek, C. Ortiz, V. J. Davisson, and D. Ben-Amotz, "Raman detection of proteomic analytes," *Analytical Chemistry*, vol. 75, no. 21, pp. 5703–5709, 2003.

[40] R. G. Larson, "In retrospect: Twenty years of drying droplets," *Nature*, vol. 550, no. 7677, pp. 466–467, 2017.

[41] R. D. Deegan, O. Bakajin, T. F. Dupont, G. Huber, S. R. Nagel, and T. A. Witten, "Capillary flow as the cause of ring stains from dried liquid drops," *Nature*, vol. 389, no. 6653, pp. 827–829, 1997.

[42] V. Kopecký Jr. and V. Baumruk, "Structure of the ring in drop coating deposited proteins and its implication for Raman spectroscopy of biomolecules," *Vibrational Spectroscopy*, vol. 42, no. 2, pp. 184–187, 2006.

[43] C. Ortiz, D. Zhang, Y. Xie, A. E. Ribbe, and D. Ben-Amotz, "Validation of the drop coating deposition Raman method for protein analysis," *Analytical Biochemistry*, vol. 353, no. 2, pp. 157–166, 2006.

[44] J. Filik and N. Stone, "Drop coating deposition Raman spectroscopy of protein mixtures," *Analyst*, vol. 132, no. 6, p. 544, 2007.

[45] G. Holzwarth, E. C. Hsu, H. S. Mosher, T. R. Faulkner, and A. Moscowitz, "Infrared circular dichroism of carbon-hydrogen and carbon-deuterium stretching modes. Calculations," *Journal of the American Chemical Society*, vol. 96, no. 1, pp. 252–253, 1974.

[46] L. A. Nafie and R. K. Dukor, "Applications of vibrational optical activity in the pharmaceutical industry," in *Applications of Vibrational Spectroscopy in Pharmaceutical Research and Development*, D. E. Pivonka, J. M. Chalmers, and P. R. Griffiths, Eds., Wiley, 2007, pp. 129–154.

[47] E. Burgueño-Tapia and P. Joseph-Nathan, "Vibrational circular dichroism: Recent advances for the assignment of the absolute configuration of natural products," *Natural Product Communications*, vol. 10, no. 10, pp. 1785–95, 2015.

[48] M. P. D. Hatfield, R. F. Murphy, and S. Lovas, "VCD spectroscopic properties of the β-hairpin forming miniprotein CLN025 in various solvents," *Biopolymers*, vol. 93, no. 5, pp. 442–450, 2010.

[49] V. Andrushchenko, D. Tsankov, M. Krasteva, H. Wieser, and P. Bouř, "Spectroscopic detection of DNA quadruplexes by vibrational circular dichroism," *Journal of the American Chemical Society*, vol. 133, no. 38, pp. 15 055–15 064, 2011.

[50] T. A. Keiderling, "Protein and peptide secondary structure and conformational determination with vibrational circular dichroism," *Current Opinion in Chemical Biology*, vol. 6, no. 5, pp. 682–688, 2002.

[51] R. Schweitzer-Stenner, "Advances in vibrational spectroscopy as a sensitive probe of peptide and protein structure – A critical review," *Vibrational Spectroscopy*, vol. 42, no. 1, pp. 98–117, 2006.

[52] K. J. Jalkanen, V. Würtz Jürgensen, A. Claussen, A. Rahim, G. M. Jensen, R. C. Wade, F. Nardi, C. Jung, I. M. Degtyarenko, R. M. Nieminen, F. Herrmann, M. Knapp-Mohammady, T. A. Niehaus, K. Frimand, and S. Suhai, "Use of vibrational spectroscopy to study protein and DNA structure, hydration, and binding of biomolecules: A combined theoretical and experimental approach," *International Journal of Quantum Chemistry*, vol. 106, no. 5, pp. 1160–1198, 2006.

[53] L. D. Barron, M. P. Bogaard, and A. D. Buckingham, "Raman-scattering of circularly polarized-light by optically-active molecules," *Journal of the American Chemical Society*, vol. 95, no. 2, pp. 603–605, 1973.

[54] L. A. Nafie, "Vibrational optical activity," *Applied Spectroscopy*, vol. 50, no. 5, 14A–26A, 1996.

[55] L. D. Barron, L. Hecht, I. H. McColl, and E. W. Blanch, "Raman optical activity comes of age," *Molecular Physics*, vol. 102, no. 8, pp. 731–744, 2004.

[56] L. D. Barron and A. D. Buckingham, "Vibrational optical activity," *Chemical Physics Letters*, vol. 492, no. 4-6, pp. 199–213, 2010.

[57] T. Fujisawa, R. L. Leverenz, M. Nagamine, C. A. Kerfeld, and M. Unno, "Raman optical activity reveals carotenoid photoactivation events in the orange carotenoid protein in solution," *Journal of the American Chemical Society*, vol. 139, no. 30, pp. 10 456–10 460, 2017.

[58] C. Mensch, A. Konijnenberg, R. Van Elzen, A. M. Lambeir, F. Sobott, and C. Johannessen, "Raman optical activity of human α-synuclein in intrinsically disordered, micelle-bound α-helical, molten globule and oligomeric β-sheet state," *Journal of Raman Spectroscopy*, vol. 48, no. 7, pp. 910–918, 2017.

[59] A. J. Hobro, M. Rouhi, G. L. Conn, and E. W. Blanch, "Raman and Raman optical activity (ROA) analysis of RNA structural motifs," *Vibrational Spectroscopy*, vol. 48, no. 1, pp. 37–43, 2008.

[60] E. W. Blanch, L. Hecht, and L. D. Barron, "Vibrational Raman optical activity of proteins, nucleic acids, and viruses," *Methods*, vol. 29, no. 2, pp. 196–209, 2003.

[61] L. D. Barron, *Molecular Light Scattering and Optical Activity*. Cambridge University Press, 2009, p. 443.

[62] I. Noda, "2DCOS and I. Three decades of two-dimensional correlation spectroscopy," *Journal of Molecular Structure*, vol. 1124, pp. 3–7, 2016.

[63] I. Noda, "Two-dimensional infrared (2-D IR) spectroscopy of synthetic and biopolymers," *Bulletin of the American Physical Society*, vol. 31, p. 520, 1986.

[64] I. Noda, "Two-dimensional infrared spectroscopy," *Journal of the American Chemical Society*, vol. 111, no. 21, pp. 8116–8118, 1989.

[65] I. Noda, "Two-Dimensional Infrared (2D IR) Spectroscopy: Theory and Applications," *Applied Spectroscopy*, vol. 44, no. 4, pp. 550–561, 1990.

[66] I. Noda and Y. Ozaki, *Two-Dimensional Correlation Spectroscopy: Applications in Vibrational and Optical Spectroscopy*. Chichester: Wiley, 2004.

[67] I. Noda, "Progress in two-dimensional (2D) correlation spectroscopy," *Journal of Molecular Structure*, vol. 799, no. 1–3, pp. 2–15, 2006.

[68] I. Noda, "Recent advancement in the field of two-dimensional correlation spectroscopy," *Journal of Molecular Structure*, vol. 883-884, pp. 2–26, 2008.

[69] Y. Park, I. Noda, and Y. M. Jung, "Novel developments and applications of two-dimensional correlation spectroscopy," *Journal of Molecular Structure*, vol. 1124, pp. 11–28, 2016.

[70] K. Pearson, "On lines and planes of closest fit to systems of points in space," *The London, Edinburgh, and Dublin Philosophical Magazine and Journal of Science*, vol. 2, no. 11, pp. 559–572, 1901.

[71] H. Hotelling, "Relations between two sets of variates," *Biometrika*, vol. 28, no. 3/4, p. 321, 1936.

[72] H. P. Singh, R. K. Gulati, and R. Gupta, "Stellar spectral classification using principal component analysis and artificial neural networks," *Monthly Notices of the Royal Astronomical Society*, vol. 295, no. 2, pp. 312–318, 1998.

[73] P. Gratier, E. Bron, M. Gerin, J. Pety, V. V. Guzman, J. Orkisz, S. Bardeau, J. R. Goicoechea, F. Le Petit, H. Liszt, K. Öberg, N. Peretto, E. Roueff, A. Sievers, and P. Tremblin, "Dissecting the molecular structure of the OrionB cloud: insight from principal component analysis," *Astronomy & Astrophysics*, vol. 599, A100, 2017.

[74] Y. He, X. Li, and X. Deng, "Discrimination of varieties of tea using near infrared spectroscopy by principal component analysis and BP model," *Journal of Food Engineering*, vol. 79, no. 4, pp. 1238–1242, 2007.

[75] D. Granato, J. S. Santos, G. B. Escher, B. L. Ferreira, and R. M. Maggio, "Use of principal component analysis (PCA) and hierarchical cluster analysis (HCA) for multivariate association between bioactive compounds and functional properties in foods: A critical perspective," *Trends in Food Science & Technology*, vol. 72, pp. 83–90, 2018.

[76] P. Antonelli, H. E. Revercomb, L. A. Sromovsky, W. L. Smith, R. O. Knuteson, D. C. Tobin, R. K. Garcia, H. B. Howell, H.-L. L. Huang, and F. A. Best, "A principal component noise filter for high spectral resolution infrared measurements," *Journal of Geophysical Research: Atmospheres*, vol. 109, no. 23, p. D23102, 2004.

[77] F. Castells, P. Laguna, L. Sörnmo, A. Bollmann, and J. M. Roig, "Principal component analysis in ECG signal processing," *EURASIP Journal on Advances in Signal Processing*, vol. 2007, no. 1, p. 074 580, 2007.

[78] A. D. Halai, A. M. Woollams, and M. A. Lambon Ralph, "Using principal component analysis to capture individual differences within a unified neuropsychological model of chronic post-stroke aphasia: Revealing the unique neural correlates of speech fluency, phonology and semantics," *Cortex*, vol. 86, pp. 275–289, 2017.

[79] E. R. Malinovski, *Factor Analysis in Chemistry*, 3rd ed. New York: Wiley, 2002.

[80] J. M. Deane, "Data reduction using principal components analysis," in *Data Handling in Science and Technology*, vol. 9, Elsevier, 1992, pp. 125–177.

[81] H. Hamaguchi, "Calibrating multichannel Raman spectrometers," *Applied Spectroscopy Reviews*, no. December 2011, pp. 37–41, 1988.

[82] C. J. Petty, G. M. Warnes, P. J. Hendra, and M. Judkins, "Relative intensity calibration of single-beam near-infrared spectrometers," *Spectrochimica Acta Part A: Molecular and Biomolecular Spectroscopy*, vol. 47, no. 9110, pp. 1179–1187, 1991.

[83] M. Fryling, C. J. Frank, and R. L. McCreery, "Intensity calibration and sensitivity comparisons for CCD/Raman spectrometers," *Applied Spectroscopy*, vol. 47, no. 12, pp. 1965–1974, 1993.

[84] E. S. Etz, S. J. Choquette, and W. S. Hurst, "Development and certification of NIST standard reference materials for relative Raman intensity calibration," *Microchimica Acta*, vol. 149, no. 3-4, pp. 175–184, 2005.

[85] V. Profant, M. Pazderková, T. Pazderka, P. Maloň, and V. Baumruk, "Relative intensity correction of Raman optical activity spectra facilitates extending the spectral region," *Journal of Raman Spectroscopy*, vol. 45, no. 7, pp. 603–609, 2014.

[86] S. Ma, X. Cao, M. Mak, A. Sadik, C. Walkner, T. B. Freedman, I. K. Lednev, R. K. Dukor, and L. A. Nafie, "Vibrational circular dichroism shows unusual sensitivity to protein fibril formation and development in solution," *Journal of the American Chemical Society*, vol. 129, no. 41, pp. 12 364–12 365, 2007.

[87] D. Kurouski, R. A. Lombardi, R. K. Dukor, I. K. Lednev, and L. A. Nafie, "Direct observation and pH control of reversed supramolecular chirality in insulin fibrils by vibrational circular dichroism," *Chemical Communications (Cambridge, England)*, vol. 46, no. 38, pp. 7154–6, 2010.

[88] G. Zhang, V. Babenko, W. Dzwolak, and T. A. Keiderling, "Dimethyl sulfoxide induced destabilization and disassembly of various structural variants of insulin fibrils monitored by vibrational circular dichroism," *Biochemistry*, vol. 54, no. 49, pp. 7193–7202, 2015.

[89] B. Martial, T. Lefèvre, and M. Auger, "Understanding amyloid fibril formation using protein fragments: structural investigations via vibrational spectroscopy and solid-state NMR," *Biophysical Reviews*, pp. 1–17, 2018.

[90] X. Lu, H. Li, J. W. Nafie, T. Pazderka, M. Pazderková, R. K. Dukor, and L. A. Nafie, "A vibrational circular dichroism microsampling accessory: Mapping enhanced vibrational circular dichroism in amyloid fibril films," *Applied Spectroscopy*, vol. 71, no. 6, pp. 1117–1126, 2017.

[91] M. W. MacArthur and J. M. Thornton, "Deviations from planarity of the peptide bond in peptides and proteins," *Journal of Molecular Biology*, vol. 264, no. 5, pp. 1180–1195, 1996.

[92] M. Pazderková, V. Profant, J. Hodačová, J. Šebestík, T. Pazderka, P. Novotná, M. Urbanová, M. Šafařík, M. Buděšínský, M. Tichý, L. Bednárová, V. Baumruk, and P. Maloň, "Nonplanar tertiary amides in rigid chiral tricyclic dilactams. Peptide group distortions and vibrational optical activity," *The Journal of Physical Chemistry B*, vol. 117, no. 33, pp. 9626–42, 2013.

[93] A. L. Jenkins, R. A. Larsen, and T. B. Williams, "Characterization of amino acids using Raman spectroscopy," *Spectrochimica Acta Part A: Molecular and Biomolecular Spectroscopy*, vol. 61, no. 7, pp. 1585–94, 2005.

[94] G. Zhu, X. Zhu, Q. Fan, and X. Wan, "Raman spectra of amino acids and their aqueous solutions," *Spectrochimica Acta Part A: Molecular and Biomolecular Spectroscopy*, vol. 78, no. 3, pp. 1187–95, 2011.

[95] N. Derbel, B. Hernández, F. Pflüger, J. Liquier, F. Geinguenaud, N. Jaïdane, Z. B. Lakhdar, and M. Ghomi, "Vibrational analysis of amino acids and short peptides in hydrated media. I. L-glycine and L-leucine," *The Journal of Physical Chemistry B*, vol. 111, no. 6, pp. 1470–7, 2007.

[96] B. Hernández, F. Pflüger, M. Nsangou, and M. Ghomi, "Vibrational analysis of amino acids and short peptides in hydrated media. IV. Amino acids with hydrophobic side chains: L-alanine, L-valine, and L-isoleucine," *The Journal of Physical Chemistry B*, vol. 113, no. 10, pp. 3169–78, 2009.

[97] B. Hernández, F. Pflüger, A. Adenier, S. G. Kruglik, and M. Ghomi, "Vibrational analysis of amino acids and short peptides in hydrated media. VIII. Amino acids with aromatic side chains: L-phenylalanine, L-tyrosine, and L-tryptophan," *The Journal of Physical Chemistry B*, vol. 114, no. 46, pp. 15 319–30, 2010.

[98] B. Hernández, F. Pflüger, N. Derbel, J. de Coninck, and M. Ghomi, "Vibrational analysis of amino acids and short peptides in hydrated media. VI. Amino acids with positively charged side chains: L-lysine and L-arginine," *The Journal of Physical Chemistry B*, vol. 114, pp. 1077–1088, 2010.

[99] F. Pflüger, B. Hernández, and M. Ghomi, "Vibrational analysis of amino acids and short peptides in hydrated media. VII. Energy landscapes, energetic and geometrical features of L-histidine with protonated and neutral side chains," *The Journal of Physical Chemistry B*, vol. 114, no. 27, pp. 9072–83, 2010.

[100] J. Kapitán, V. Baumruk, V. Kopecký Jr., R. Pohl, and P. Bouř, "Proline zwitterion dynamics in solution, glass, and crystalline state," *Journal of the American Chemical Society*, vol. 128, no. 41, pp. 13 451–62, 2006.

[101] T. Pazderka and V. Kopecký, "Drop coating deposition Raman spectroscopy of proteinogenic amino acids compared with their solution and crystalline state," *Spectrochimica Acta Part A: Molecular and Biomolecular Spectroscopy*, vol. 185, pp. 207–216, 2017.

[102] R. Botta, A. Rajanikanth, and C. Bansal, "Surface enhanced Raman scattering Studies of L-amino acids adsorbed on silver nanoclusters," *Chemical Physics Letters*, vol. 618, pp. 14–19, 2015.

[103] S. M. Rolfe, M. R. Patel, I. Gilmour, K. Olsson-Francis, and T. J. Ringrose, "Defining multiple characteristic Raman bands of α-amino acids as biomarkers for planetary missions using a statistical method," *Origins of Life and Evolution of Biospheres*, vol. 46, no. 2-3, pp. 323–346, 2016.

[104] L. D. Barron, "Structure and behaviour of biomolecules from Raman optical activity," *Current Opinion in Structural Biology*, vol. 16, no. 5, pp. 638–643, 2006.

[105] P. L. Polavarapu and C. Zhao, "Vibrational circular dichroism: A new spectroscopic tool for biomolecular structural determination," *Fresenius' Journal of Analytical Chemistry*, vol. 366, no. 6–7, pp. 727–734, 2000.

[106] L. Ashton, B. Czarnik-Matusewicz, and E. W. Blanch, "Application of two-dimensional correlation analysis to Raman optical activity," *Journal of Molecular Structure*, vol. 799, no. 1–3, pp. 61–71, 2006.

[107] T. Pazderka and V. Kopecký Jr., "Two-dimensional correlation analysis of Raman optical activity – Basic rules and data treatment," *Vibrational Spectroscopy*, vol. 60, pp. 193–199, 2012.

[108] T. Pazderka, "Studium dynamiky proteinů pomocí optické spektroskopie," Diploma Thesis, Charles Univesity, Prague, 2009.

[109] Y. M. Jung, B. Czarnik-Matusewicz, and Y. Ozaki, "Two-dimensional infrared, two-dimensional Raman, and two-dimensional infrared and Raman heterospectral correlation studies of secondary structure of beta-lactoglobulin in buffer solutions," *The Journal of Physical Chemistry B*, vol. 104, pp. 7812–7817, 2000.

[110] H. C. Choi, Y. M. Jung, I. Noda, and S. B. Kim, "A study of the mechanism of the electrochemical reaction of lithium with CoO by two-dimensional soft x-ray absorption spectroscopy (2D XAS), 2D Raman, and 2D heterospectral XAS—Raman correlation analysis," *The Journal of Physical Chemistry B*, vol. 107, no. 24, pp. 5806–5811, 2003.

[111] Y. Wu, J.-H. Jiang, and Y. Ozaki, "A new possibility of generalized two-dimensional correlation spectroscopy: Hybrid two-dimensional correlation spectroscopy," *The Journal of Physical Chemistry A*, vol. 106, no. 11, pp. 2422–2429, 2002.

[112] L. Zhang, I. Noda, and Y. Wu, "Concatenated two-dimensional correlation analysis: A new possibility for generalized two-dimensional correlation spectroscopy and its application to the examination of process reversibility," *Applied Spectroscopy*, vol. 64, no. 3, pp. 343–350, 2010.

[113] Y. Wu, L. Zhang, and I. Noda, "Improvement of "concatenated" two-dimensional correlation analysis and its new potential applications on the quantitative evaluation of the process reversibility under different perturbations," *Vibrational Spectroscopy*, vol. 60, pp. 220–225, 2012.

[114] I. Noda, "Projection two-dimensional correlation analysis," *Journal of Molecular Structure*, vol. 974, no. 1–3, pp. 116–126, 2010.

[115] M. Mecozzi and E. Sturchio, "Effects of essential oil treatments on the secondary protein structure of *Vicia faba*: A mid-infrared spectroscopic study supported by two-dimensional correlation analysis," *Spectrochimica Acta Part A: Molecular and Biomolecular Spectroscopy*, vol. 137, pp. 90–98, 2015.

[116] R. Acquistucci, V. Melini, S. Cecconi, and M. Mecozzi, "Evaluation of rheological properties of four italian rice samples and starch thereof by RVA and FTIR spectroscopy supported by double two-dimensional correlation analysis: Evidence of lipid–carbohydrate interactions," *Cereal Chemistry Journal*, vol. 93, no. 5, pp. 456–464, 2016.

[117] W. McNavage and H.-L. Dai, "Two-dimensional cross-spectral correlation analysis and its application to time-resolved Fourier transform emission spectra of transient radicals," *The Journal of Chemical Physics*, vol. 123, no. 18, p. 184 104, 2005.

[118] M. R. Langlois and J. R. Delanghe, "Biological and clinical significance of haptoglobin polymorphism in humans," *Clinical Chemistry*, vol. 42, no. 10, 1996.

[119] C. B. F. Andersen, M. Torvund-Jensen, M. J. Nielsen, C. L. P. de Oliveira, H.-P. Hersleth, N. H. Andersen, J. S. Pedersen, G. R. Andersen, and S. K. Moestrup, "Structure of the haptoglobin-haemoglobin complex," *Nature*, vol. 489, no. 7416, pp. 456–9, 2012.

[120] R. Ettrich, W. Brandt, V. Kopecký Jr., V. Baumruk, K. Hofbauerová, and Z. Pavlíček, "Study of chaperone-like activity of human haptoglobin: conformational changes under heat shock conditions and localization of interaction sites," *Biological Chemistry*, vol. 383, no. 10, pp. 1667–1676, 2002.

[121] N. Maeda and O. Smithies, "The evolution of multigene families: Human haptoglobin genes," *Annual Review of Genetics*, vol. 20, no. 1, pp. 81–108, 1986.

[122] F. Polticelli, A. Bocedi, G. Minervini, and P. Ascenzi, "Human haptoglobin structure and function–a molecular modelling study," *The FEBS Journal*, vol. 275, no. 22, pp. 5648–5656, 2008.

[123] T. Okazaki and T. Nagai, "Difference in hemoglobin-binding ability of polymers among haptoglobin phenotypes," *Clinical Chemistry*, vol. 43, no. 10, pp. 2012–2013, 1997.

[124] V. Kopecký Jr., R. Ettrich, T. Pazderka, K. Hofbauerová, D. Řeha, and V. Baumruk, "Influence of ligand binding on structure and thermostability of human α_1-acid glycoprotein," *Journal of Molecular Recognition*, vol. 29, no. 2, pp. 70–79, 2016.

[125] S. Urien, Y. Giroud, R.-S. Tsai, P.-A. Carrupt, F. Brée, B. Testa, and J.-P. Tillement, "Mechanism of ligand binding to α_1-acid glycoprotein (orosomucoid): correlated thermodynamic factors and molecular parameters of polarity," *Biochemical Journal*, vol. 306, pp. 545–549, 1995.

[126] T. J. Measey and R. Schweitzer-Stenner, "Vibrational circular dichroism as a probe of fibrillogenesis: The origin of the anomalous intensity enhancement of amyloid-like fibrils," *Journal of the American Chemical Society*, vol. 133, no. 4, pp. 1066–1076, 2011.

[127] W. R. W. Welch, J. Kubelka, and T. A. Keiderling, "Infrared, vibrational circular dichroism, and Raman spectral simulations for β-sheet structures with various isotopic labels, interstrand, and stacking arrangements using density functional theory," *The Journal of Physical Chemistry B*, vol. 117, no. 36, pp. 10 343–58, 2013.

[128] M. Pazderková, T. Pazderka, M. Shanmugasundaram, R. K. Dukor, I. K. Lednev, and L. A. Nafie, "Origin of enhanced VCD in amyloid fibril spectra: Effect of deuteriation and pH," *Chirality*, vol. 29, pp. 469–475, 2017.

List of Abbreviations

2DCoS two-dimensional correlation spectroscopy

AGP α_1-acid glycoprotein

DCDR drop coating deposition Raman

FT-IR Fourier transformed infrared spectroscopy

HEWL hen egg white lysozyme

HI human insulin

Hp human haptoglobin

ICP incident circular polarization

IR infrared

LCP left circularly polarized

NMR nuclear magnetic resonance

PCA principal component analysis

PPII poly-proline II helix

RCP right circularly polarized

ROA Raman optical activity

SERS surface-enhanced Raman scattering

SNR signal to noise ratio

VCD vibrational circular dichroism

VOA vibrational optical activity

List of Publications

- T. Pazderka and V. Kopecký Jr., "Two-dimensional correlation analysis of Raman optical activity – Basic rules and data treatment," *Vibrational Spectroscopy*, vol. 60, pp. 193–199, 2012

  Author's contribution: Complete simulation of the spectra and calculations of two-dimensional spectra, participation on writing of the manuscript.

- M. Pazderková, V. Profant, J. Hodačová, J. Šebestík, T. Pazderka, P. Novotná, M. Urbanová, M. Šafařík, M. Buděšínský, M. Tichý, L. Bednárová, V. Baumruk, and P. Maloň, "Nonplanar tertiary amides in rigid chiral tricyclic dilactams. Peptide group distortions and vibrational optical activity," *The Journal of Physical Chemistry B*, vol. 117, no. 33, pp. 9626–42, 2013

  Author's contribution: Contribution to analysis of experimental and theoretical data and preparation of ROA experiment.

- V. Profant, M. Pazderková, T. Pazderka, P. Maloň, and V. Baumruk, "Relative intensity correction of Raman optical activity spectra facilitates extending the spectral region," *Journal of Raman Spectroscopy*, vol. 45, no. 7, pp. 603–609, 2014

  Author's contribution: Major contribution to measurements, participation on analysis of experimental data and writing of the manuscript.

- V. Kopecký Jr., R. Ettrich, T. Pazderka, K. Hofbauerová, D. Řeha, and V. Baumruk, "Influence of ligand binding on structure and thermostability of human α_1-acid glycoprotein," *Journal of Molecular Recognition*, vol. 29, no. 2, pp. 70–79, 2016

  Author's contribution: Measurements of Raman spectra, subsequent analysis and writing of the corresponding part of the manuscript.

- T. Pazderka and V. Kopecký, "Drop coating deposition Raman spectroscopy of proteinogenic amino acids compared with their solution and crystalline state," *Spectrochimica Acta Part A: Molecular and Biomolecular Spectroscopy*, vol. 185, pp. 207–216, 2017

  Author's contribution: Complete measurements of experimental data, major contribution to subsequent analysis and writing of the manuscript.

- X. Lu, H. Li, J. W. Nafie, T. Pazderka, M. Pazderková, R. K. Dukor, and L. A. Nafie, "A vibrational circular dichroism microsampling accessory:

Mapping enhanced vibrational circular dichroism in amyloid fibril films," *Applied Spectroscopy*, vol. 71, no. 6, pp. 1117–1126, 2017

Author's contribution: Building of the VCD microsampling instrument, measurements and subsequent data analysis.

- M. Pazderková, T. Pazderka, M. Shanmugasundaram, R. K. Dukor, I. K. Lednev, and L. A. Nafie, "Origin of enhanced VCD in amyloid fibril spectra: Effect of deuteriation and pH," *Chirality*, vol. 29, pp. 469–475, 2017

  Author's contribution: Major contribution to measurements and analysis of experimental data. Participation on writing of the manuscript.

- T. Pazderka and V. Kopecký, "Protein hetero-sample two-dimensional correlation analysis: A case of human haptoglobin phenotypes," *submitted*

  Author's contribution: Complete measurements of experimental data, major contribution to subsequent analysis, contribution to writing of the manuscript.

1. Relative intensity correction of Raman optical activity spectra facilitates extending the spectral region

2. A vibrational circular dichroism microsampling accessory: Mapping enhanced vibrational circular dichroism in amyloid fibril films

3. Nonplanar tertiary amides in rigid chiral tricyclic dilactams. Peptide group distortions and vibrational optical activity

3.1 Supplementary data

4. Drop coating deposition Raman spectroscopy of proteinogenic amino acids compared with their solution and crystalline state

4.1 Supplementary data

5. Two-dimensional correlation analysis of Raman optical activity – Basic rules and data treatment

5.1 Supplementary data

6. Protein hetero-sample two-dimensional correlation analysis: A case of human haptoglobin phenotypes

7. Influence of ligand binding on structure and thermostability of human α_1-acid glycoprotein

7.1 Supplementary data

8. Origin of enhanced VCD in amyloid fibril spectra: Effect of deuteriation and pH